RAM ROBOTICS AND MECHATRONICS

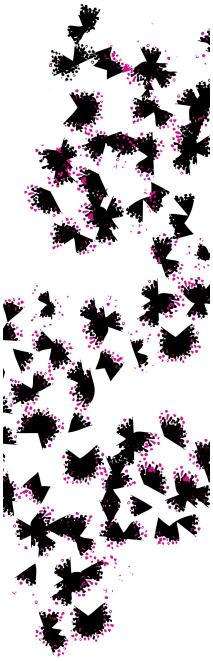

Design, fabrication and characterisation of a force sensitive sensor from inhomogenous 3D printed material

M.G.T. (Maaike) Laagland

BSc Report

Committee:
Prof.dr.ir. G.J.M. Krijnen
G.J. Wolterink, MSc
Ing. R.G.P. Sanders
Dr.ir. B.J.F. van Beijnum

July 2018

023RAM2018
Robotics and Mechatronics
EE-Math-CS
University of Twente
P.O. Box 217
7500 AE Enschede
The Netherlands

UNIVERSITY OF TWENTE.

MIRA CTIT
BIOMEDICAL TECHNOLOGY AND TECHNICAL MEDICINE

Executive summary

The objective of this report is developing a 3D printed capacitive force sensitive sensor made from flexible conductive carbon based thermoplastic polyurethane (ETPU). In earlier research a resistance between printed layers in a 3D printed material is found, which could be due to an inhomogeneous distribution of conductive carbon particles.

These inhomogeneous properties are unwanted in existing 3D printed applications, but can also be used to create new applications, as is done in this research. The functioning of the capacitive force sensor is be based on the use of the inhomogeneous properties of the material. For the capactive sensor to function as a capacitor, two conducting plates should be close to each other separated with a dielectric material. Because the sensor only consists of ETPU it can not function solely as a capacitor, it will have a parallel and serial resistance as well. So, ETPU should function as both the conductive plates as the dielectric. The conductive plates are the areas with the highest concentration of carbon particles, which is assumed is in the center of the material. What results in the surrounding material containing a lower concentration carbon particles. Here is where the percolation theory comes along. The percolation theory states that there is a turning point in the relation of percentage of carbon particles and conductivity of the material. This turning point is the percentage of carbon particles where the conductivity substantially increases. Because carbon particles make the material more brittle, the least possible amount of carbon particles is infused in the material, which caused that the percentage carbon particles is probably around the turning point. Areas with a slightly smaller concentration of carbon particles, could cause a lot less conductivity than areas with a slightly higher concentration of carbon particles. This causes the areas with a slightly smaller percentage carbon particles to function as the dielectric, which is the reason two layers of 3D printed material could function as a capacitor, with a serial and parallel resistor. These inhomogeneous properties could be caused by the fabrication process of the filament or during the printing process. The cause is not yet known.

The biomedical relevance is in prosthetics. When an external force is applied to the sensor, the capacitance will change. This change could be linked to a specific force change, which would make the force sensor measure the amount of force that is applied. The use of this force sensor could be in thimbles for prosthetic hands to give feedback to the person wearing the prosthetic to what kind of force is exerted.

The force sensor will be printed with use of a technique called fused deposition modeling (FDM). In FDM a spool of filament is loaded into the printer where it is heated up and deposit on a platform in a pre-set pattern. After filament is printed, it immediately hardens. When one layer is finished, the next layer will be printed on top. The filament will not blend with the previously printed filament, which causes the filament to keep its inhomogeneous properties. The printer used is a FlashForge Creater Pro with a flexion extruder head which allows the printer to print two materials at the same time.

The technology behind the capacitive sensing relays on a measured change in capacitance between the printed layers when external force is applied. The force sensor is compared to the functioning of a parallel plate capacitor, but with a few alterations. The surface area used in the formula is replaced by the total volume of the sensor and a parallel and serial resistor is added in the electrical circuit of the sensor. The impedance, capacitance and resistance are measured with an LCR meter. For the transition from impedance to resistance and capacitance a frequency response model is created, this model is be fitted over the measured data and helps determining the capacitance and resistance of the test structures and force sensors.

After all the requirements were gathered, it was clear that for the transition from a idea to a prototype research is required. The impacts of printing orientations will be compared, the contact resistances of contact interfaces and the functioning of the two-layered force sensor. The parallel resistance of different types of printing orientation will be compared to gain insight about the differences originating in the printing process and the contact resistances of the contact interfaces will be measured. These will be tested on one-layered test structures.

For the infill patterns a four point measurement is used to exclude the influence of the contact resistance and to solely measure the parallel resistance. The three infill patterns compared are perpendicular, parallel with a brim and parallel without a brim relative to the contact interfaces. Every type of infill is at least printed and measured 5 times. The prediction is that the parallel resistance of the perpendicular oriented infill is the lowest, because it would be the easiest for the current to follow the path with the

highest concentration of carbon particles. The parallel oriented infill patterns will be more difficult for the current to flow through. This is confirmed by the results of the measurements. The perpendicular oriented infill patterns causes the lowest parallel resistance, parallel oriented infill patterns with a brim the second lowest parallel resistance and the parallel oriented infill patterns without a brim caused the highest parallel resistance. So the perpendicular oriented infill is used while printing the two-layered sensor.

The measurements regarding the contact resistances used two and four point measurements on the same test structure to calculate the contact interface. Four types of contact interfaces were compared, two which required heat in the mounting process, namely a header pin and stripped copper wire. The other two did not affect the material in the mounting process. These connections are a copper clip and a braid structure which was printed with the sensor. Every contact interface is at least printed and measured 3 times. The measured data showed that the copper clips have the lowest contact resistance. The braid structure has the highest contact resistance. The recommendations when using contact interfaces in further research is to use clips, it will not damage the material because no heat is used in the mounting process and the connection is easier to mount.

The two-layered force sensor are two times fabricated, one consisting of two layers with the same printing orientation and one consisting of two layers with a different printing orientation. A four point measurement is applied to solely focus on the change in resistance due to the applied force. The contact interfaces used to connect the sensor to a electrical source in both layers is mounted in a way that only one layer is connected. A surface of $10\,\mathrm{mm}$ by $10\,\mathrm{mm}$ is the real sensor, this consists of two electrically loaded layers. A tip of a linear actuator applies an external force to this surface. The expectation was an increase in capacitance when external force was applied but the results of the force sensor with the same printing orientation show a decrease in capacitance with steps of $50\,\mathrm{pF}$ by a force difference of $2\,\mathrm{N}$. The results of the sensor made of two layers with a different orientation also show a decrease in capacitance but on a smaller, about scale$5\,\mathrm{pF}$ by a force difference of $2\,\mathrm{N}$. Based on the observations and measurements the two-layered force sensor with the same printing orientation show potential to function as a capacitive force sensor. However, further research needs to be done.

Contents

Chapter 1

Introduction

> If a picture is worth thousand words, a prototype is worth thousand pictures.
>
> *IDEO*

1.1 Research goal

Since the early 80's the world has gained a new way of manufacturing where material is added instead of removed. Hence the name, additive manufacturing, more commonly known as '3D printing'. As 3D printing is a relative new technique, there is still a lot to learn about the process and improvement needed. The most available 3D printing process is called Fused Deposition Modeling (FDM). Fused deposition modeling builds an object by depositing melted material in a pre-set pattern layer-by-layer [1]. This way of 3D printing works mostly as desired but causes unwanted side effects. In research conducted by B. Eijking use is made of Fused Deposition Modeling where multiple layers of conductive thermoplastic polyurethane filament were printed. B. Eijking discovered a resistance between these layers [2]. This measured resistance provides information about the structure and conductance of the printed filament, namely that not all the current passes by default through all layers. This is only merely an unwanted side-effect, but instead of trying to prevent it, it can be used to create new applications. The resistance between the layers makes that these printed layers from conductive filament in principle can function as a capacitor. As is the objective of this report, to develop a 3D printed capacitive force sensitive sensor made from multiple layers of carbon doped thermoplastic polyurethane (ETPU). The functioning of the sensor will be based on the use of the inhomogeneous properties. Inhomogeneous properties are the properties in the printed material which cause the resistance between the layers. This will be further explained in Section 1.3.

1.2 Printing a capacitive force sensitive sensor

Little research is done regarding 3D printed capactive sensors, one of the few is the research done is by Schouten et al. [3], who developed a 3D printed flexible capacitive force sensor. This sensor consists of a parallel plate capacitor build from regular and conductive thermoplastic polyurethane. Due to an applied sinusoidal force, the capacitance in the sensor changed, which makes that the sensor functions as a capacitor. A second research is done by Saari et al. [4] who created a composite 3D printed capacitive force sensor with the use of fiber encapsulation additive manufacturing. For the dielectric material thermoplastic elastomer additive manufacturing is used. The capacitive sensor consists of a 3D printed rigid frame with copper wires as electrodes which are embedded during the printing, this emulates a parallel plate capacitor.

Both of the researches made use of multiple materials with one material being conductive and one material non-conductive. Making use of the inhomogeneous properties of the conductive printed material,

the non-conductive material will not be necessary to make the sensor function as a capacitor. Secondly, different kinds of contact interfaces were used in both sensors. Interfaces connect the sensor to an electrical source. In the research of Schouten et al. is made use of 4 shielded cables with no further elaboration on the properties of the cables and in the research by Saari et al. copper wires are used as the interface which are embedded during printing. The way a contact interface is embedded in a sensor causes a contact resistance which could affect the conductance measurements. And final, both sensors consist of multiple layers without taking a possible resistance or capacitance between the layers into account. What could be concluded is that no research regarding 3D printed capacitive sensors made from one inhomogeneous material. Besides the sensor itself, the contact resistance of different contact interfaces on capacitive force sensors have not been researched earlier.

1.3 Inhomogeneous material

As stated earlier, in research done by B. Eijking is a unexpected resistance found which originates between multiple printed layers of conductive carbon doped thermoplastic polyurethane. The cause of the existence of this resistance could be due to two reasons.

First the adhesion between the printed layers. In FDM printing the object is built layer-by-layer so when the first layer is printed, the printing bed moves down in the negative z direction or the extruder head moves up in the positive z direction and the extruder starts printing the second layer. In theory, the printed filament that is being printed melts together with the already printed layer which causes bonding of the two layers. But in reality, these two layers will not always melt together perfectly. This shows in the bond strength between the printed layers, this bond strength is always lower than the base strength, in the x and y direction, of the material. One of the reasons of the layers not blending together uniformly, is due to the nozzle being located closer to the printer tabletop than the diameter of the filament. This causes the filament to spread out to a shape which is more like an oval than the round form the filament initially had, as seen in Fig. 1.2, and causes the surface to be wavy. When a new layer is printed on top of the wavy surface, the height differences causes the strength of the adhesion to vary over the surface [1]. Due to the adhesion strength between the layers being lower than the strength in the x and y direction, it can be interred that the layers aren't properly melted together in the z direction which could cause an isolated conductance between the layers.

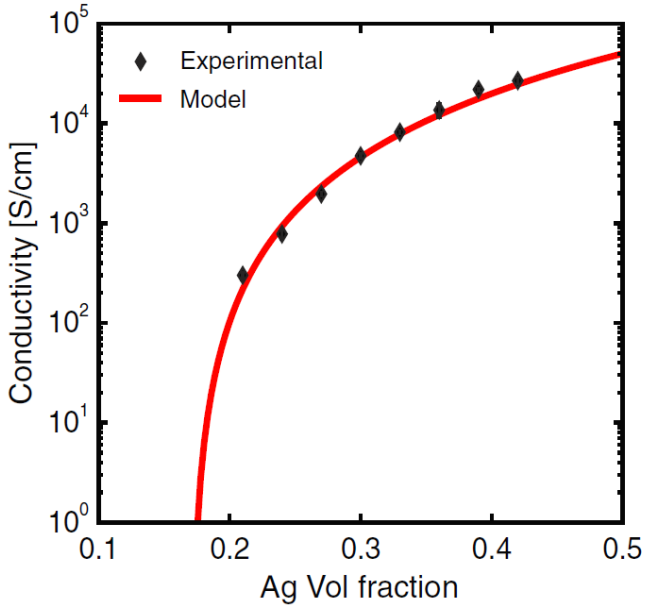

Figure 1.1: Electrical conductivity of AgTPU composite as a function of silver flake content. Red line is a fit to the data (black) using the power-law relationship [7].

The second option has to do with the composition of the filament. As earlier stated, the material used for

the sensor is carbon doped thermoplastic polyurethane (ETPU). ETPU consists of a compound material with a carbon black filler which causes the material to become somewhat electrically conductive [5]. The carbon black is an added material, which makes that it is not distributed uniformly in the material. This could cause regions in the material with a higher or lower concentration. When the concentration carbon black at near the contact areas is low and the concentration is high in the center of the printed filament, as visualized in Fig. 1.3, it could cause the measured resistance. This theory is in line with the percolation theory. The percolation theory describes the increase of the resistivity of the material related to the percentage or fraction of the conductive filler This is done by increasing the probability of current being transferred by electrically contacting particles which start to form networks at higher concentration [6].

An example of a research where the percolation theory is used is done by A. Valentine et al, where soft electronics via hybrid 3D printing were created. Hybrid 3D printing combines direct ink writing of conductive and dielectric elastomeric materials which are printed in a pre-set layout and passive and electrical components are also integrated. These components are then interconnected via printed conductive traces. This creates soft electronic devices. To do so conductive electrode ink is produced, where silver flakes were added to pure thermoplastic polyurethane ink. Afterwards the conductivity of the silver thermoplastic urethane as a function of the volume fraction of the silver flakes was plotted, which is shown in Fig. 1.1. Here is seen that there is no conductivity in the material with fractions silver flakes lower than 0.18. When the fraction increases from 0.18, the conductivity substantially increases as well. [7].

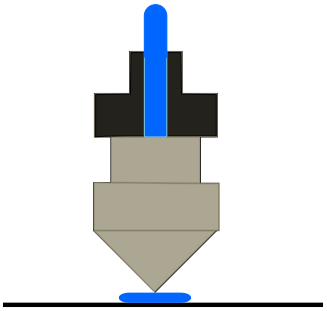

Figure 1.2: Sketch of a nozzle extruding filament onto the printer bed.

As earlier stated, the percolation theory also applies to the ETPU. An easy fix would be to add more carbon particles, but a too high carbon concentration in the ETPU leads to a more brittle material [8], which probably causes that as little carbon particles as possible is mixed in the thermoplastic polyurethane. This causes the concentration of carbon particles to be around the turning point. When the carbon particles are not distributed well, it could cause areas with a slightly lower or higher concentration of carbon particles. As seen in Fig. 1.1, a slightly lower concentration could lead to significantly lower conductivity. If the outer areas of the filament, near the contact area, have a slightly lower concentration of carbon particles, it could explain the measured unexpectedly high resistance between the layers.

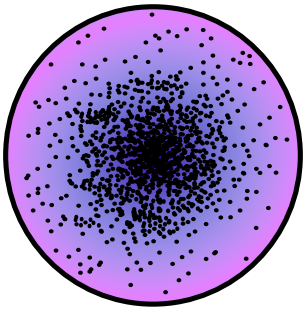

Figure 1.3: Sketch of assumed cross section of a filament with the the black dots representing carbon particles.

The big question remains, what causes this inhomogeneous distribution of carbon particles? Multiple

explanations are possible, starting with the inhomogeneous distribution already being present n the filament, as visualized in Fig. 1.3. This would mean that the process of creating the filament causes the carbon particles distribution. Unfortunately there is no information about the production process of ETPU available so this would only be a speculation.

An other possibility is that the fabrication has no impact on the distribution of carbon particles but the inhomogeneous distribution develops during the printing process. During 3D printing, filament is first heated up to its melting point and then deposited on the printing bed where it cools down and solidifies. Because the nozzle is located close to the bed, the printed filament changes from a round to an oval shape (as seen in Fig. 1.2. The change of the form of the filament could change the distribution of carbon particles, which would make the printed filament to look like Fig. 1.4.

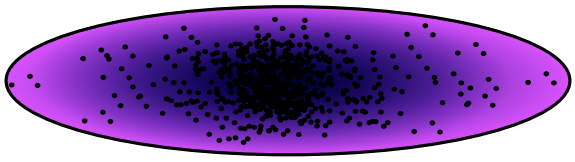

Figure 1.4: Sketch of assumed cross section of a printed filament with the the black dots being carbon particles.

During this research, it will be assumed that the high contact-resistance between the printed layers is due to the inhomogeneous distribution of carbon particles in combination with the earlier stated percolation theory.

1.4 Biomedical relevance

When an external force is applied to the sensor, the capacitance will change. This change could be linked to a specific force change, so the force sensor could measure the amount of force that is applied. The use of this force sensor could be in thimbles for prosthetic hands to give feedback to the person wearing the prosthetic to what kind of force is exerted by the prosthetic hand. For example, to pick up an egg without breaking it. There are multiple advantages in making these thimbles with the use of additive manufacturing. First, the thimbles can be easily customized. Second, complexity is cheap in additive manufacturing, so it can be interesting money wise and third, the finished product, the thimbles, could be quickly realized. [3].

1.5 Thesis outline

This report consists of 8 chapters with this chapter being an introduction to the research with general information. In chapter 2 the technology behind the force sensor is discussed. Chapter 3 focuses on the the requirements and designing a model. Chapter 4 elaborates on the fabrication of the force sensor and in chapter 5 the experimental setup is discussed. In chapter 6 the results are gathered following by a discussion in chapter 7 and finally, the conclusion can be found in chapter 8 where recommendations for further research are stated.

Chapter 2

Technology

This chapter will focus on the technology needed to make the sensor function as a capacitive force sensor. The technology used for printing the sensor is discussed and also the technology behind capacitive sensing.

2.1 Fused deposition modelling

For the sensors to be printed, a technique called fused deposition modelling (FDM) is used. In FDM a spool of thermoplastic filament is loaded into the printer where it is heated up by a nozzle until the melting point of the material is reached. The melted material is then extruded in a pre-set pattern and deposited on a platform where it cools down and solidifies. After a layer is finished, the next layer will be printed on top of the already printed layer. This process will continue until the printed model is finished [1]. Because of the almost immediate hardening of the filament, the filament will not blend with the already printed filament. This causes the filament to hold its own mechanical properties. The printed model can be looked at as one very long filament printed in a desired pattern, like a knit sweater made from wool. This can be seen in Fig. 2.2, the infill pattern of a printed structure is easily distinguished.

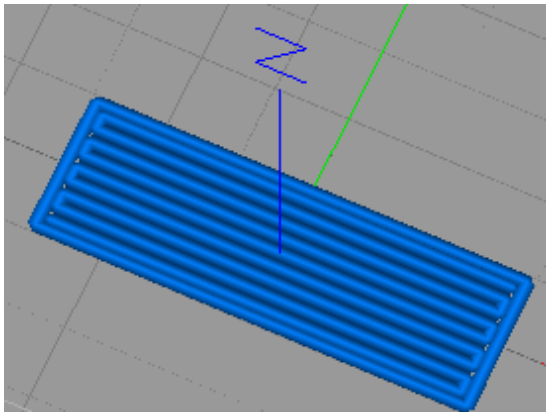

Figure 2.1: The design and infill pattern of a test structure.

Figure 2.2: A picture of the printed test structure.

2.2 Capactive sensing

The force sensitive sensor is based on a measured change in capacitance between the printed layers when external force is applied. Because the height of the printed layers will be significantly smaller than the surface area ($0.07\,\mu m$ versus $100\,mm^2$), and the sensor will consist of two layers, the sensor will be

treated as a parallel plate capacitor. A sketch of a parallel plate capacitor is shown in Fig. 2.3 with the corresponding equation Eq. (2.1). Here C is the capacitance, A the surface area of the plates, d the separation between the two conducting plates, ϵ_r the relative dielectric constant and ϵ_o the permittivity of free space.

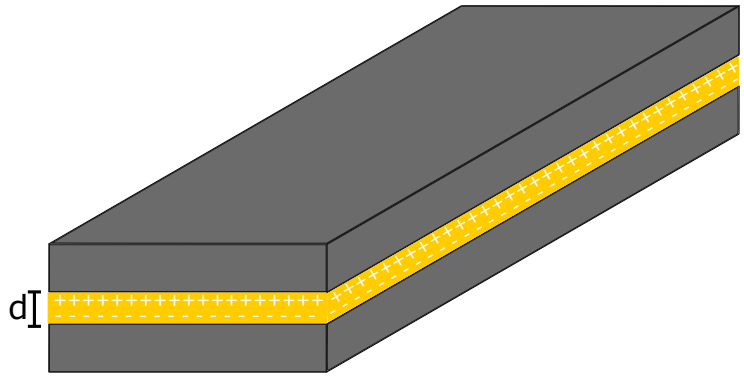

Figure 2.3: A standard parallel plate capacitor

$$C = \frac{A\epsilon_r\epsilon_o}{d} \tag{2.1}$$

Until this point a standard capacitor is described, but the sensor which will be created in this research is not a standard capacitor. The main difference is the material, the sensor will consist of only carbon doped thermoplastic polyurethane.

This material will act as both the conductive material and the dielectric, a sketch of a cross section of the sensor is seen in Fig. 2.4. The capacitance change will be due to the change in distance between the centers with a high concentration of conductive carbon particles. This makes that the sensor does not work like a normal capacitor, there are a few differences.

When looked at the Poisson ratio of thermoplastic polyurethane, an average Poisson's ratio of 0.48 is assumed [9]. The Poisson ratio can predict the change in width and length that accompany an elongation. Because the ratio is near to 0.5, the total volume of the sensor will not change when an external force is applied to the sensor. This causes the formula for capacitance change to be altered, which is shown in Eq. (2.2). Where V is the total volume [3].

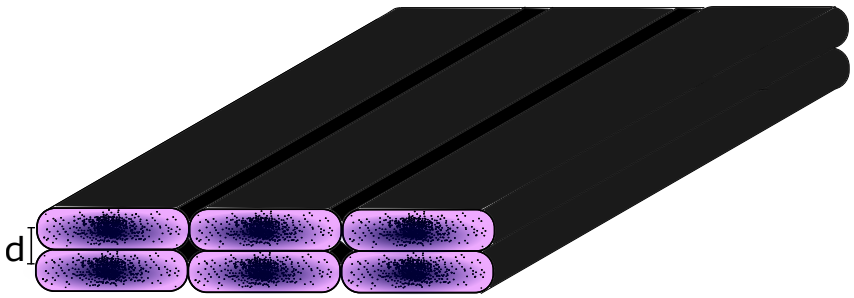

Figure 2.4: Cross section of three strands printed filament with the assumption of distribution of carbon particles, which will function as a capacitor.

$$C = \frac{A\epsilon_r\epsilon_o}{d} = \frac{V\epsilon_r\epsilon_o}{d^2} \tag{2.2}$$

The second difference are the electrical circuits. For a normal working capacitor the corresponding circuit will only contain a variable capacitor, as seen in Fig. 2.5. The circuit of the force sensor made

from ETPU contains more elements, as seen in Fig. 2.6. Due to the lack of a pure dielectric, current will flow from one layer to another. This is supported in earlier research by B. Eijking, where a resistance was measured between the layers [2]. Therefore a parallel resistor is added. The parallel resistance is also due to the resistance between the printed filament in one layer. Because the layer is printed in a meandering pre-set pattern a resistance originates between the printed lines, as is shown in Fig. 2.4. The resistance of the core material is the serial resistance in the circuit. The contact resistance of the contact interfaces will also show up in the series resistance. The circuit Fig. 2.6 will be used to make a model to determine the capacitance and resistivity of the force sensor.

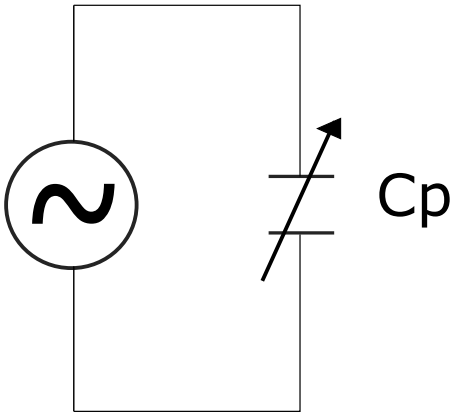

Figure 2.5: Circuit for a simple capacitor.

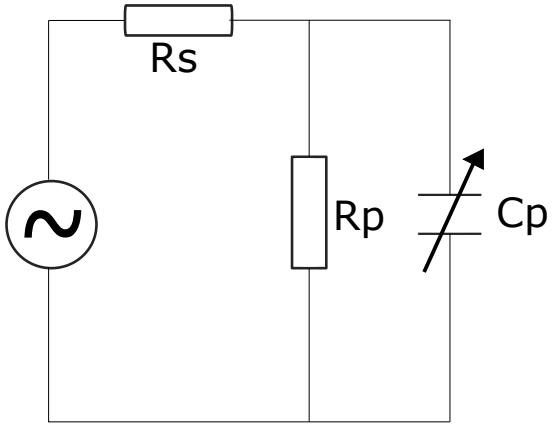

Figure 2.6: Circuit for the force sensor.

2.3 Conclusion

FDM printing will be used as the printing technique. Interesting for the force sensor is the immediate hardening of the filament, which causes the filament to not blend in with the already printed filament and to keep its mechanical properties. For the capactive sensing the formula Eq. (2.2) will be used to predict the behaviour of the force sensor. An increase in capacity when external force is applied is expected. This formula is slightly different from a standard parallel plate capacitor because the Poisson ratio of ETPU is approximately 0.5. Another difference between the standard capacitor and the force sensor is the electrical circuit. A series and parallel resistor are added. The series resistance is the resistance of the core material and the contact resistance and the parallel resistance is the resistance between printed the filament and the layers. The circuits shown in Fig. 2.6 will be used to make models to determine the capacitance and resistance of the force sensor.

Chapter 3

Design

The first steps in fabricating a capacitive force sensor are gathering the requirements for the sensor and determining what research needs to be done. This research will be further thought out and a plan of action will be made.

3.1 Requirements for the force sensor

Material

- The distance between the two plates should be able to differ. This can be done by using flexible materials for the force sensor so when external force is applied, the volume of the sensor will stay the same but it will gain surface and lose height.
- The force sensor should operate as a capacitor without adding a dielectric material, the material should act as a dielectric itself.
- The material should be soft flexible materials which can be used in biomedical applications.

Measurement setup

- The force which will be applied has to be a homogeneous force-distribution with equal pressure on the entire surface.
- Beside the actuator tip, the surface of the force sensor should be as flat as possible so that the actuator can distribute the force uniformly.

Characteristics of the force sensor

- The series resistance of the core material should be as low as possible.
- The parallel resistance between the layers should be as large as possible and the resistance between the filament in one layer should be as low as possible.

Interface

- The force sensor needs to be connected to a wire.
- The interface must interfere as little as possible with the structure of the 3D printed sensing areas.
- The contact resistance of the interfaces should be as low as possible

The transition from an idea to a prototype requires research, as can be seen in the lack of knowledge in the requirements. The requirements regarding 'characteristics' of the force sensor , 'interface' and part of the 'measurement setup' are met by designing, printing and testing the one-layered test structures. These testing structures will consist of one-layered structures where the parallel resistance is measured and one-layered testing structures where the contact resistance and impact of different types of interfaces is measured. These results will contribute to the design and fabrication of the two-layered capacitive force sensor.

3.2 One-layered test structures

3.2.1 Four point measurement

The one-layered test structure will be used to determine the series resistivity over one printed layer. To make sure only the parallel resistance is measured and not the contact resistance of the interfaces, a four point measurement is used.

During a four point measurement two current leads are connected to the outer side of the test structure where the current flows through the whole test structure. The voltage is measured through a second set of test leads which are located on the inner side, as is shown in Fig. 3.1. Due to the high impedance of the voltmeter, almost no current flows through the voltage leads, which causes the voltage drop over the measured surface to be negligible. Because the voltage drop is negligible, the contact resistances are not included when measuring the impedance citefour.

The interfaces used for this four point measurement are header pins which are connected to a copper wire. The voltage pins will be mounted 10 mm apart, which makes that the measured surface is 100 mm^2. In all measurements header pins are used as contact interfaces for consistency, with every header pin being the exact same size (a square surface of $0.6\,\mathrm{mm}$ by $0.6\,\mathrm{mm}$). The header pins will be mounted to the material by melting them into the material, which is done by heating the header pin which causes the material surrounding the header pin to melt which encapsulates the header pin.

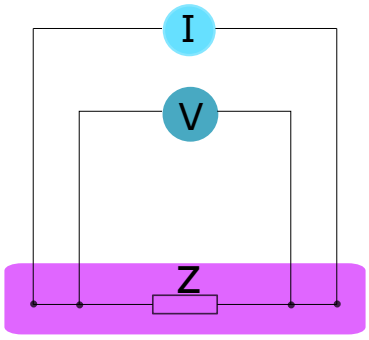

Figure 3.1: Sketch of four point measurement with the purple being the conductive material.

3.2.2 Design

For the one-layered test structures a simple design is made. As seen in the requirements, the parallel resistance should be as low as possible. The parallel resistance is among other things caused by the infill pattern of the printed layers. Multiple infill patterns are possible, but there is chosen to compare perpendicular oriented infill, parallel oriented infill with a brim, parallel oriented infill without a brim which are shown in Fig. 3.2, Fig. 3.3 and Fig. 3.4. When filament is printed, it almost immediately hardens. This causes the filament to keep its properties, which include the inhomogeneous distribution of carbon particles (as seen in Section 1.3). When current flows through a printed sensor, the current will most likely follow the path with the highest concentration of carbon particles, the center of the filament. If this is the the case, Fig. 3.2 would have the lowest parallel resistance and would be the best infill to use in the two-layered sensor. To measure the parallel resistance of the multiple infill patterns, the infill patterns shown in Fig. 3.2, Fig. 3.3 and Fig. 3.4 will be printed as a one-layered text structure with the CAD model shown in Fig. 3.5.

Because the layer height of 3D printed filament is very small, namely $200\,\mu\mathrm{m}$, the one-layered test structures will be printed onto Kapton tape to make the test structures more stable and durable.

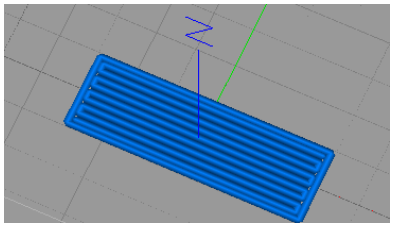

Figure 3.2: Perpendicular oriented infill pattern.

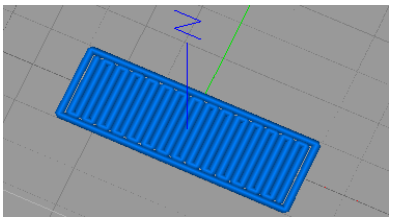

Figure 3.3: Parallel oriented infill pattern with a brim.

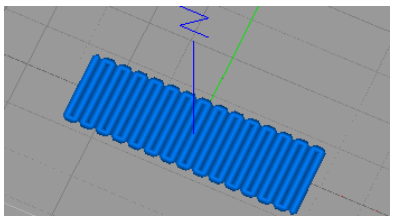

Figure 3.4: Parallel oriented infill pattern without a brim.

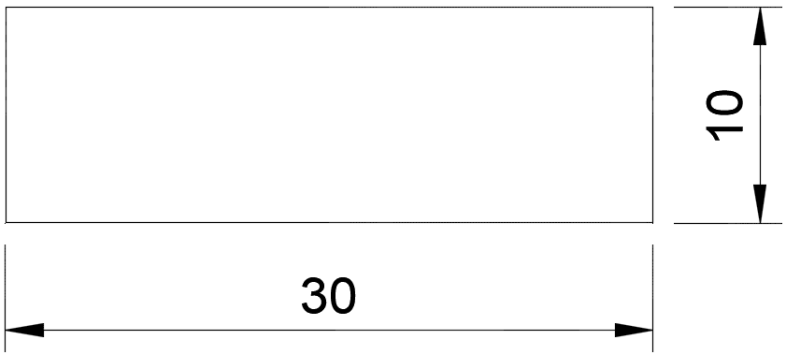

Figure 3.5: Drawing of CAD model of the one-layered test structure. The dimensions are in millimeters and the height of the structure is 0.2 mm.

3.2.3 Interfaces

Multiple methods are available for connecting a wire to the force sensor. These can be divided into two categories.

1. Interfaces which are mounted after the printing process without affecting the material.
2. Interfaces which are mounted after the printing process which do affect the material.

Interfaces from both categories will be fabricated, tested and compared. To create consistency, the interfaces will be tested on test structures with the same oriented infill, namely perpendicular.

Category one: interfaces which do not affect the material of the force sensor

Clips
A method to make a connection is by clipping conductive alligator clips with a smooth toothless beak onto the force sensor. A copper wire can be soldered onto this alligator clip. To test these clips, a simple one-layered test structure are printed where the clips can be clipped onto.

Braid
By adding two times three strands of material, a braid can be added to the sensor, as is shown in Fig. 3.6. When this test structure is printed, copper wire will be stripped and wrapped around the strands which leaves three strands covered with copper wire. These three strands will be braided as well. The printing orientation is shown in Fig. 3.7.

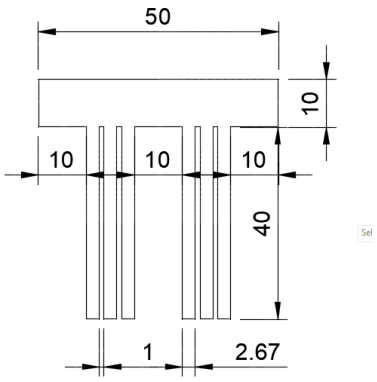

Figure 3.6: Fusion360 model of the test structure.

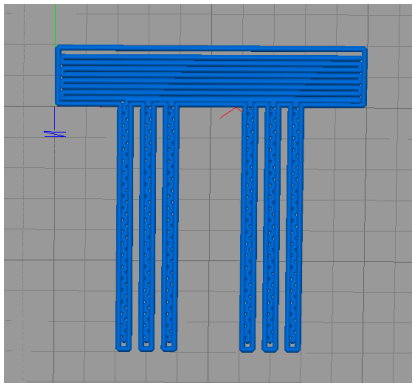

Figure 3.7: The test structure with the printing orientation.

Category two: interfaces which do affect the material of the force sensor

Header pin
As stated earlier, a header pin is an efficient way of connecting a wire to the force sensor. To test the functioning of a header pin as an interface, printed one-layered test structures are needed. In these test structures four header pins are melted. This is done by using a soldering iron.

Copper wire
For copper wire to function as an interface, it will be stripped and melted into the force sensor by using a soldering iron. To test the functioning of stripped copper wire as an interface, printed one-layered test structures are needed. Four copper wires will be melted into these test structures.

3.3 Two-layered force sensor

3.3.1 Design

Two test structures will be printed with different printing orientations. The first one with two layers which contain the same printing orientation, the one with the lowest resistance which is measured on the one-layered test structure, as seen in Fig. 3.9. The second force sensor will have two layers with different printing orientations, one perpendicular and one parallel, as seen in Fig. 3.10. The effect of these layers on top of each other will be compared.

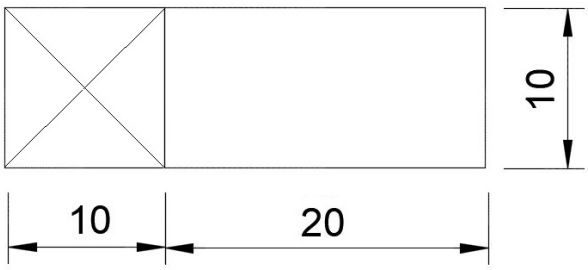

(a) Layer one of two.

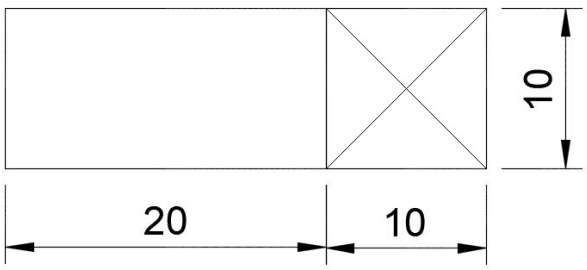

(b) Layer two of two.

Figure 3.8: Drawing of the CAD model of the two-layered force sensor with the dimensions in millimeters and the height of the structure is 0.2 mm. The ares with the cross represents the dielectric material and the open areas represent the carbon filled thermoplastic polyutherane.

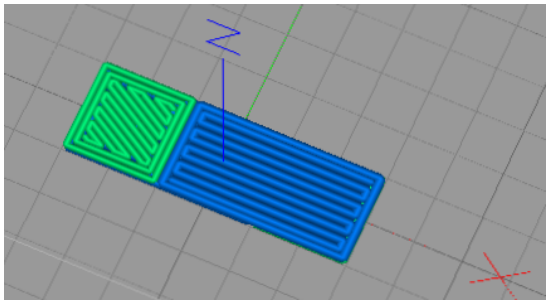

(a) Layer one of two

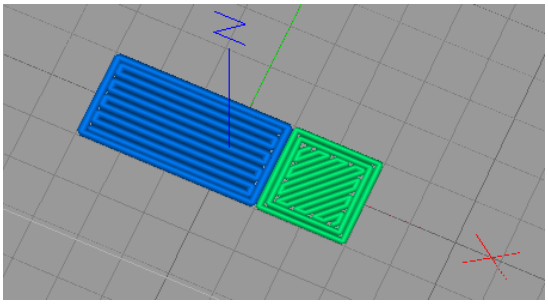

(b) Layer two of two

Figure 3.9: A slicer model of the same oriented printed two-layered force sensor.

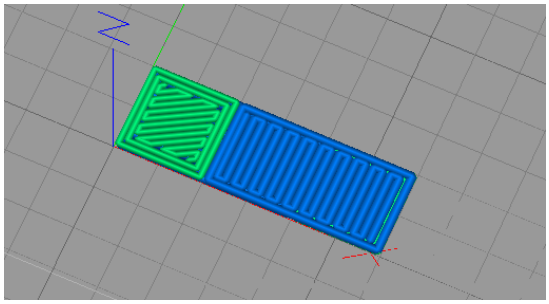

(a) Layer one of two

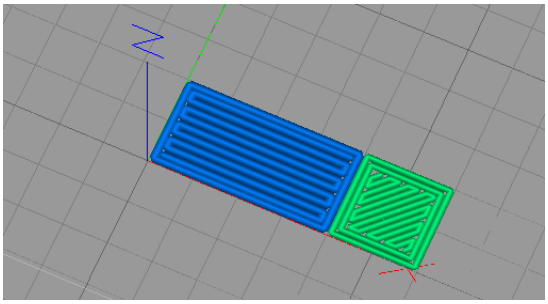

(b) Layer two of two

Figure 3.10: A slicer model of the different oriented printed two-layered force sensor.

3.3.2 Four point measurement

The two-layered force sensor will also make use of a four point measurement to eliminate the contact resistance, as is explained in Section 3.2.1. During these measurements, the force sensor will use stripped copper wires as an interface. These stripped wires will be molten into the material by heating the material around the copper wire which causes the copper wire to be embedded into the material. Both interfaces cause an increase in the height of the force sensor, but copper wire causes the smallest increase.

The layers in the force sensor need to be independently electrically connected, this will be done by adding dielectric material to the sensor. As can be seen in in Fig. 3.9 and Fig. 3.10, this material is added in a way that the interfaces can be mounted without the layer underneath interfering. The result is that only in the middle part the force sensor consists of two layers of printed carbon filled thermoplastic polyurethane which makes it the most important part of the sensor. The external force will be applied to this part which causes the capacitance change over the force sensor.

3.4 Interfaces

3.4.1 Four point measurement versus two point measurement

For the contact resistance to be determined, four and two point measurements are performed. The set up is seen in Fig. 3.11 en Fig. 3.12.

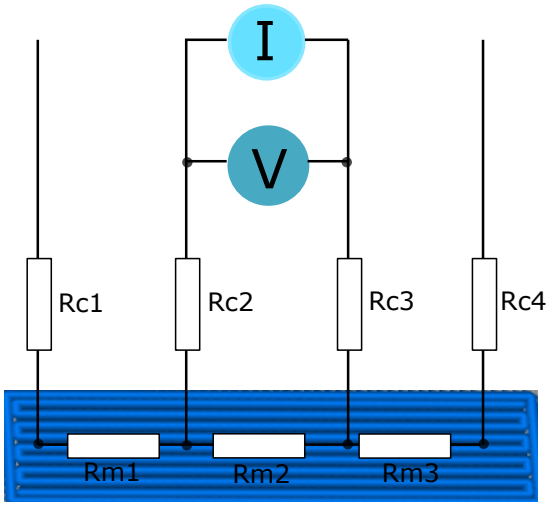

Figure 3.11: Measurement setup of a two point measurement.

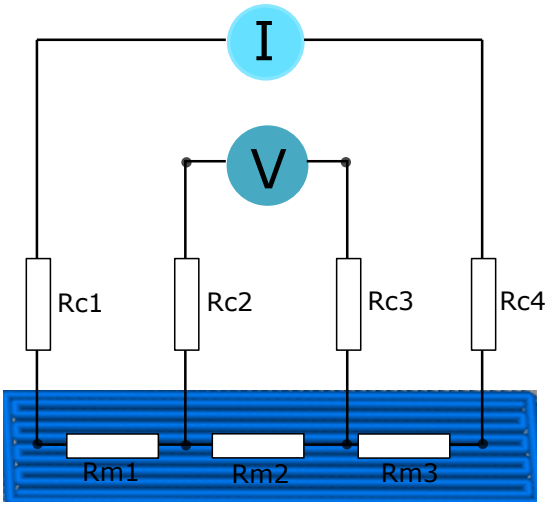

Figure 3.12: Measurement setup of a four point measurement.

The two point measurement (R_2p) contain two contact resistances, R_{c2} and R_{c4}. The four point measurement (R_4p) makes sure that no current goes through R_{c2} and R_{c3}, so only the material resistance R_{m2} is measured. The contact resistance of one connection is estimated by Eq. (3.1) [6].

$$R_c = \frac{R_{c2} + R_{c3}}{2} = \frac{R_2p - R_4p}{2} \tag{3.1}$$

This equation will be used to calculate the contact resistances of the interfaces.

3.5 Conclusion

After setting up the requirements for the force sensor, a lack of knowledge was quickly noticed. For making a capacitive force sensor function, research needs to be performed on the parallel resistance and the contact resistance of the material and interfaces. The parallel resistance is among other things caused by the infill pattern so three types of infill patterns will be compared. Four types of interfaces will be compared. These measurements will be preformed on one-layered test structures with the use of a four point measurements. In the measurements regarding the parallel resistance, it causes the contact resistance to be neglected so only the parallel resistance will be measured. In the measurements regarding contact interfaces is the other way around, here only the contact resistance needs to be measured. This will be done with a two point measurements and a four point measurements together to filter out the contact resistance. These results will be used in the design and fabrication of the force sensor.

Chapter 4

Fabrication

This chapter will focus on the materials and printer used to fabricate the test structures and force sensors.

4.1 Materials used

4.1.1 Conductive material

Carbon doped thermoplastic polyurethane
The conductive material used for the force sensor is thermoplastic polyurethane, this is a flexible material. The brand name of the used material is ETPU. The type used is PI-ETPU 95-250 Carbon Black. The recommended printing temperature range is 200 °C to 230 °C. The volume resistivity is be below 800 Ω cm [11].

Copper wire
The copper wire used for making a connection to the force sensor is Flexivolt-E wire made from copper with a PVC jacket. It contains 26 strands with a diameter of 0.07 mm and a total external diameter of 1 mm.[13].

Clips
The clips used for to measure the contact resistance are BU-34M micro-alligator copper clips. These clips have a surface area of 5 mm by 2 mm [14].

Header pins
The header pins used are standard header pins and have a square surface of 0.6 mm by 0.6 mm.

4.1.2 Non conductive material

Thermoplastic polyurethane
As seen in Section 3.3.1, for some parts of the force sensor thermoplastic polyurethane filament is used. The brand name of the used material is Ninajaflex. The recommended printing temperature range is 210 °C to 240 °C [12].

Polyamide film
Polyamide film is used to print the one-layered test structures onto. It functions also as an insulator for the two-layered force sensors. The brand name of the used material is Kapton. Kapton tape is made from polyamide film with a silicone adhesive. Kapton tape is compatible with a wide temperature range from −269 °C to 260 °C [15].

4.2 3D printer

The printer used for printing the force sensors is a FlashForge Creator Pro [16], as shown in Fig. 4.1. Due to the flexible materials that are printed, the printer is equipped with a flexion extruder from Diabase Engineering [17]. The extruder is equipped with two nozzles, which allows the printer to print 2 different materials at the same time. The transition of one material to another causes sometimes problems due to leaking of the nozzle. To prevent this leaking a brush is installed in the printer which wipes the nozzle before switching materials. The layers are printed with a layer height of 200 µm and a printing infill of 100%. The printing temperatures for the materials are 230 °C for ETPU and 220 °C for Ninjaflex, while the print bed is kept at a temperature of 50 °C

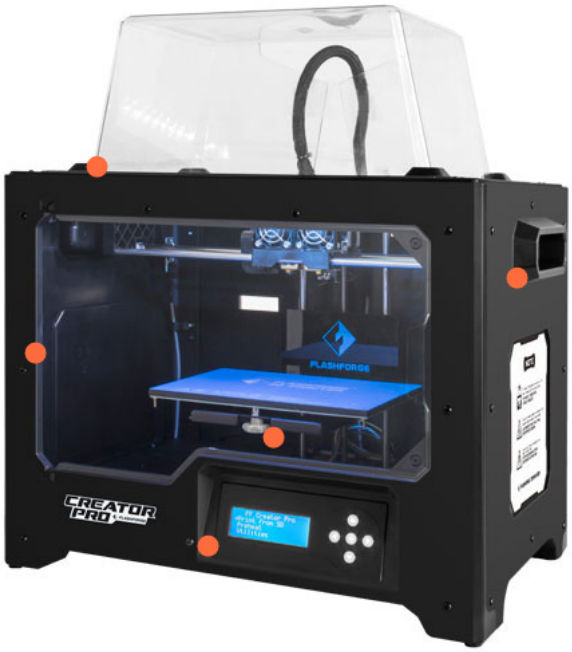

Figure 4.1: Picture of the used printer, a FlashForge Creator Pro.

4.3 Finished prints

One-layered test structures

Images of the finished test structures with the different infill patterns can be seen in Fig. 4.2, Fig. 4.3, Fig. 4.4. All the used test structures for measuring parallel resistance can be found in Appendix A.

Figure 4.2: Perpendicular oriented infill pattern.

Figure 4.3: Parallel oriented infill pattern with a brim.

Figure 4.4: Parallel oriented infill pattern without a brim.

Interfaces

Images of the finished test structures for the different interfaces can be found in Fig. 4.5, Fig. 4.6, Fig. 4.8 and Fig. 4.7. All the used test structures for measuring contact resistance can be found in Section 8.1.

Figure 4.5: Header pin interface.

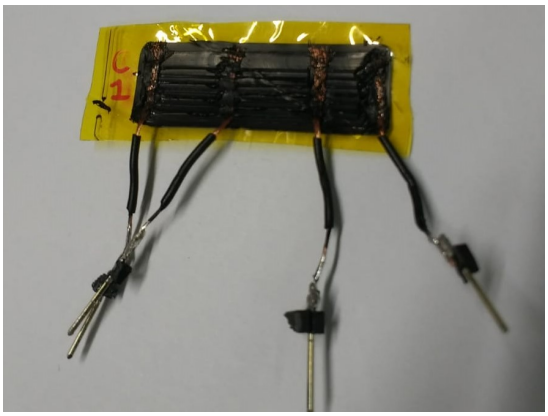

Figure 4.6: Copper wire interface.

Figure 4.7: Braid interface.

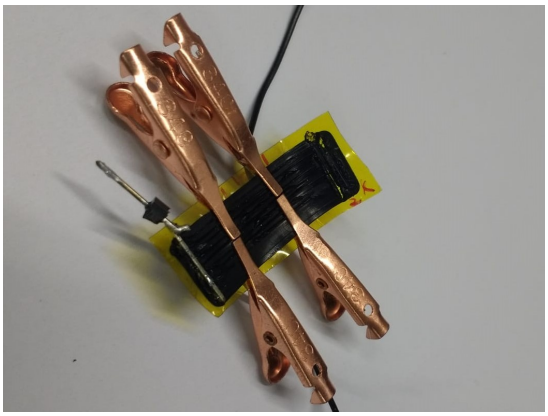

Figure 4.8: Copper clips interface.

Two-layered force sensors

An image of the finished two-layered force sensors can be seen in Fig. 4.9.

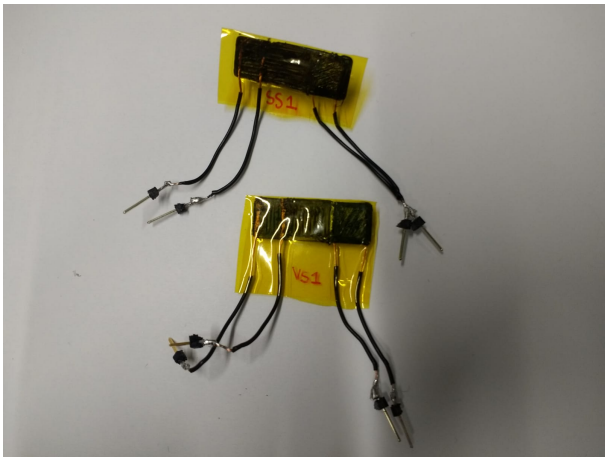

Figure 4.9: The two two-layered force sensors.

4.4 Conclusion

Both conductive and non conductive material are used in fabricating the sensors and the contact interfaces. The materials in combination with a printer with the right settings created nice test structures and force sensors. No further problems or revelations were encountered in this chapter.

Chapter 5

Experimental setup

Now the test structures and force sensors are fabricated, they are ready to be measured. This will be done with the use of an LCR meter for impedance measurements and a linear actuator which applies force during the measurements. This chapter will focus on the experimental setup of the measurements and how the values for resistance and capacitance are determined.

5.1 Impedance measurements

For the impedance measurements of the test structures, the HP 4284A Precision LCR Meter is used. An LCR meter measures the inductance, capacitance and resistance of electronic components. The LCR meter makes use of a four-terminal pair measurements, as is shown in Fig. 5.1 [18]. In this figure four leads are shown, these are the current (L_{cur} and H_{cur}) and potential leads (L_{pot} and H_{pot}). These leads are connected to the DUT. DUT stands for device under test, which is in this case the test structure or the sensor.

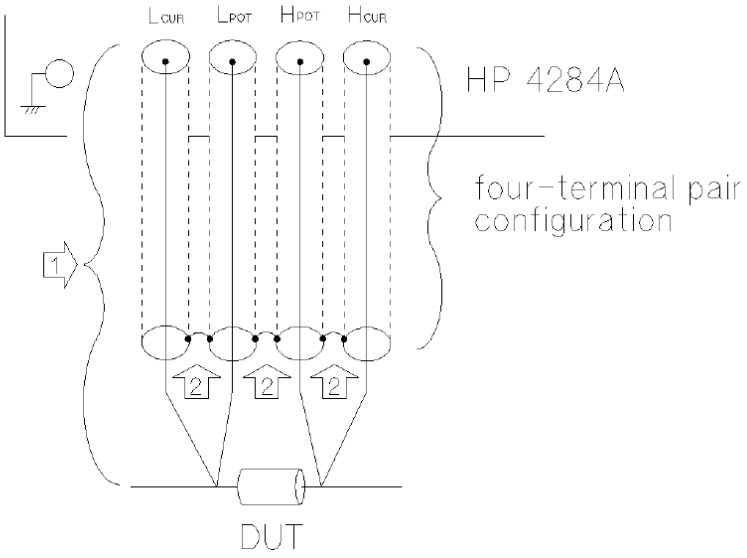

Figure 5.1: Measurement contacts of the LCR meter. [18]

5.1.1 One-layered test structures

For measurements with the one-layered test structures the impedance (Z) and phase of impedance (θ) is measured by the LCR meter while the LCR meter runs through a range of frequencies between 20 Hz and 1 MHz. The impedance and phase shift can be plotted on a logarithmic scale plot to the frequencies.

From impedance to resistance and capacitance

To determine the capacitance and resistance values of the test structures more than the impedance measurements are needed. Namely the electrical circuit of the test structure and the corresponding frequency response. The frequency response will be fitted over the impedance plot, which is acquired by the measurements. When the perfect fit is reached, the capacitance and resistance values can be determined.

For the frequency response of the parallel impedance the electrical circuit seen in Fig. 5.2 is used.

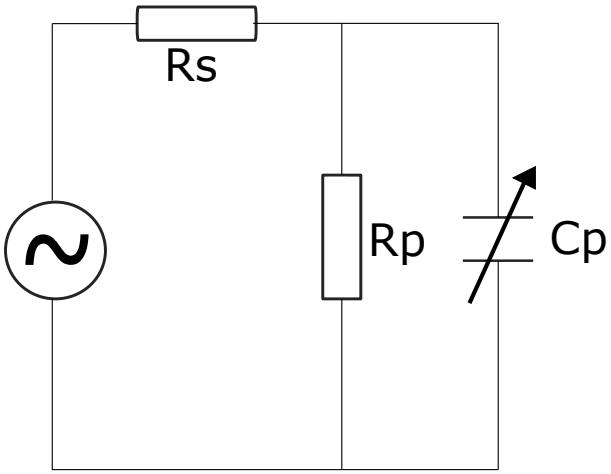

Figure 5.2: The circuit for a one-layered test structure.

To determine the value of the the parallel impedance which comes forward from Fig. 5.2, the elements are first determined.

$$Z_r = R_p \tag{5.1}$$

$$Z_c = \frac{1}{j\omega C} \tag{5.2}$$

Where ω is the angular frequency of the sinusoidal signal, C the capacitance and R_p the parallel resistance. Because for the measurements frequency is used instead of angular frequency, the impedance of the capacitor is given by Eq. (5.3). For parallel impedance, the function Eq. (5.4) is used, when combined with Eq. (5.1) and Eq. (5.2), the parallel impedance Eq. (5.6) is determined.

$$Z_c = \frac{1}{j2\pi fC} \tag{5.3}$$

$$\frac{1}{Z_p} = \frac{1}{Z_r} + \frac{1}{Z_c} \tag{5.4}$$

$$\frac{1}{Z_p} = \frac{1}{\frac{1}{j2\pi fC}} + \frac{1}{R_p} \tag{5.5}$$

$$Z_p = \frac{R_p}{j2\pi fCR_p + 1} \tag{5.6}$$

This parallel impedance can be represented as a frequency response. An example of a potential frequency response is shown in Fig. 5.3.

A frequency response gives information about the parallel resistance and and helps to determine these values.

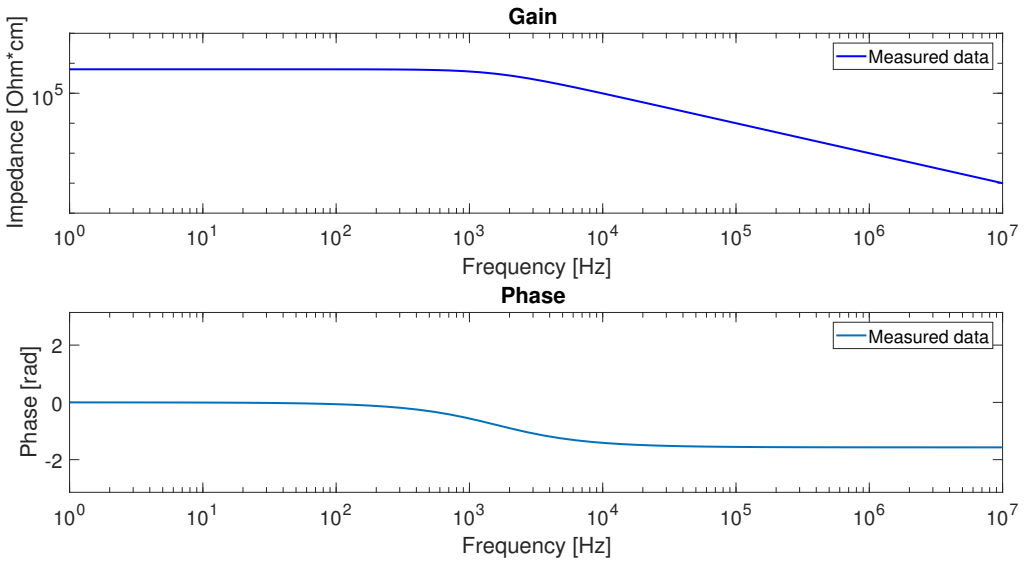

Figure 5.3: Frequency response of a parallel RC circuit with R_p=630 kΩ and C=1 nF. This is a simulated model.

The corner frequency f_c is the frequency where the magnitude of the impedance starts to decrease. As can be seen in Eq. (5.8), the corner frequency is depends on the value of the resistance and capacitance. When the corner frequency is known, the capacitance value can be determined with the use of Eq. (5.8).

Before the corner frequency, the value of the magnitude is stable. This is the value of the parallel resistance R_p+R_s. [19].

$$\omega_c = \frac{1}{R_p C} \tag{5.7}$$

$$f_c = \frac{\omega_c}{2\pi} = \frac{1}{2\pi R_p C} \tag{5.8}$$

So, a frequency response is plotted and fitted over the measured impedance plot. With the use of the corner frequency and the value of the magnitude before the corner frequency, the values for the capacitance and resistance can be determined.

5.2 Interfaces

For measuring the contact interfaces, the capacitance of the sensors will be ignored and only the resistance will be determined. By low frequencies the impendance only shows R_s+R_p. When the frequency increases and reaches its corner frequency, the impedance decreases with a slope of 20 dB. When the frequency becomes very high, the capacitance becomes a short circuit and only the R_s is left. Because the LCR meter can only measure up to 1 MHz the flattening of impedance is not seen in the results. So for measuring the contact resistance, the value before the corner frequency f_c is taking and the mean of impedance between the frequencies from 20 to 100 Hz is measured. In four point measurements the R_s is ignored and only the R_p is measured and in two point measurements both R_s+R_p are measured so with the use of Eq. (3.1) the R_s, the contact resistance, can be determined.

5.3 Lineair actuator

For the two-layered force sensors a linear actuator is used to apply a force onto the sensor, when simultaneously measuring the capacitance and resistance of the force sensor by the HP 4284A Precision LCR Meter. The used actuator is the SMAC LCA25-050-15F [20]. The actuator is able to apply force between 1 N and 10 N in steps of 1 N. The tip of the actuator will exert the force so it should have the exact same dimensions of the force sensor, namely 10 mm by 10 mm. Therefore a tip is made from a PVC with the same dimensions. The material of the tip should deform little under pressure. To make sure the tips meets this requirement, the tip will be tested and the deformation will me measured. This will be compared with the deformation of the original tip of the actuator. A picture of the total setup is shown in Fig. 5.4.

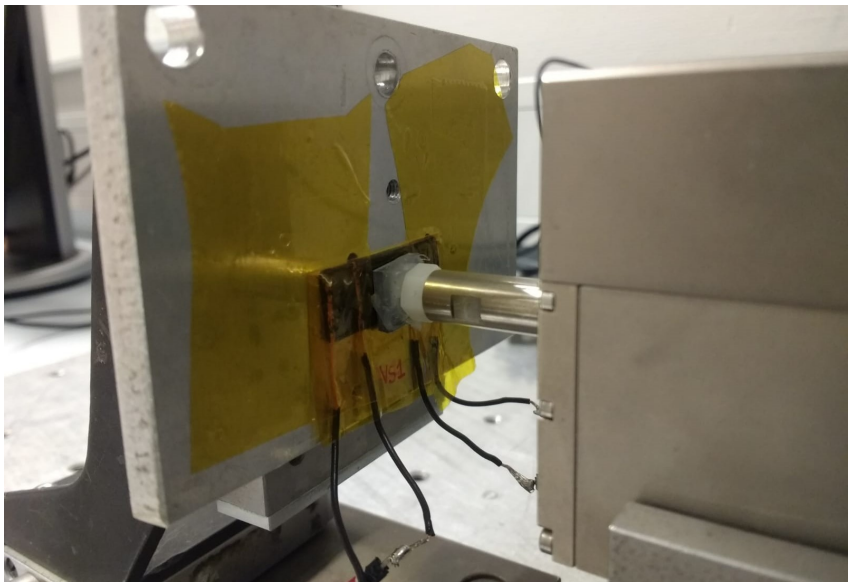

Figure 5.4: Picture of the SMAC setup with the two-layered force sensor taped on the bed with polyamide film for stability.

5.4 Conclusion

The experimental setup of the measurements regarding one-layered test structures and two-layered force sensors consists of an LCR meter and a linear actuator. The LCR meter performs impedance measurements. These measurements are fitted with a frequency response of the electrical circuit of the force sensor. The frequency response is based on the parallel impedance shown in Fig. 5.3. The plot of the frequency response helps determining the values for the resistance and capacitance with the use of the corner frequency. The corner frequency is the frequency at which the magnitude of the impedance starts to decrease. The formula is shown in Eq. (5.8) where is seen that it depends on the value of resistance and capacitance. For the measurements regarding the contact interfaces only the value of the magnitude before the corner frequency is used, which is the same value as the series resistance plus the parallel resistance. When performing four and two point measurements, the value of the series resistance can be determined. For the measurements with the force sensor, a linear actuator will apply force from 1 N to 10 N in steps of 2 N.

Chapter 6

Results

In this chapter will the results of the measurements be shown and discussed. On the one-layered test structure measurements regarding the parallel resistance and contact resistance are done. The capacitance and resistance of two-layered force sensors are measured while applying force. And finally the deformation of the actuator tip is measured.

6.1 One-layered test structures

For the one-layered test structures in total 24 test structures were printed, 9 with a parallel oriented infill pattern with a brim, 5 with a parallel oriented infill pattern without a brim and 10 with a perpendicular oriented infill pattern. The number of printed test structures because multiple sensors were damaged by the soldering iron or were not printed correctly.

To exclude the influence of the printer, all test structures should be printed at the same time. Unfortunately the printer could only print 10 test structures at the same time due to a shortage of space on the printing bed. So decided is to print half of the test structures with the parallel oriented infill with a brim and half of the test structures with the perpendicular oriented infill at the same time. This print process is repeated two times. The test structures with a parallel oriented infill without a brim were printed separately because the decision to measure this printing orientation was made when the other two oriented infill test structures were already printed. The test structures are printed on polyamide film with a print layer height of $200\,\mu m$.

The test structures are measured in a four point measurement with the middle two voltage leads $1\,cm$ apart. Because the connections are mounted by hand, this distance differs throughout the test structure. To compensate for these differences, the distance between the voltage strands is measured and the impedance values per measured test structure are divided by this test structure specific value. This means the unit resistance is changed to resistivity.

The LCR meter measured the impedance and phase at 50 frequencies between the $20\,Hz$ and $1\,MHz$ MHz in two sweeps. These two sweeps are converted to one plot, where the mean of the two sweeps is taken.

All measurements done are shown in Fig. 6.1, Fig. 6.2 and Fig. 6.3. At low frequencies the structures behaves similar but when the frequency increases and reaches $10\,kHz$, the magnitude of the impedance and phase stop acting similar to the frequency response. This causes the structures to have a different slope than the slope of the frequency response. Around $100\,kHz$ the data starts acting similar again. To make sure this behaviour is not caused by the LCR meter, a capacitor and resistor were soldered together and measured with the same LCR setup, this is shown in Fig. 6.4. When the measured data of the combined capacitor and resistor would also behave different around $10\,kHz$, the behaviour was probably caused by the LCR meter. But as is shown in Fig. 6.5, the model fits perfectly over the measured data. So, the LCR meter functions perfectly and the reason for the odd behaviour around Fig. 6.5 lays in the test structures.

In the figures Fig. 6.1, Fig. 6.2 and Fig. 6.3 is seen that the measured data does not overlap well, even though it is all measured on sensors with the same oriented infill pattern. To compare to what degree the data is overlapping, error bars are measured. Error bars indicate the error and uncertainty of the measurements. These error bars of the measured data are shown in Appendix B. From these plots is concluded that the perpendicular oriented printed test structures have the smallest error bar which means this infill orientation causes the most consistent data.

For every infill orientation the mean of all the data is taken and plotted into one graph to compare the infill orientations, this is shown in Fig. 6.6. The values for the capacitance and resistance of the infill orientations with compensation for the distance between the contact interfaces are shown in Table 6.1. The plots where the frequency response is fitted onto the measured data, to acquire these values, can be found in Appendix C.

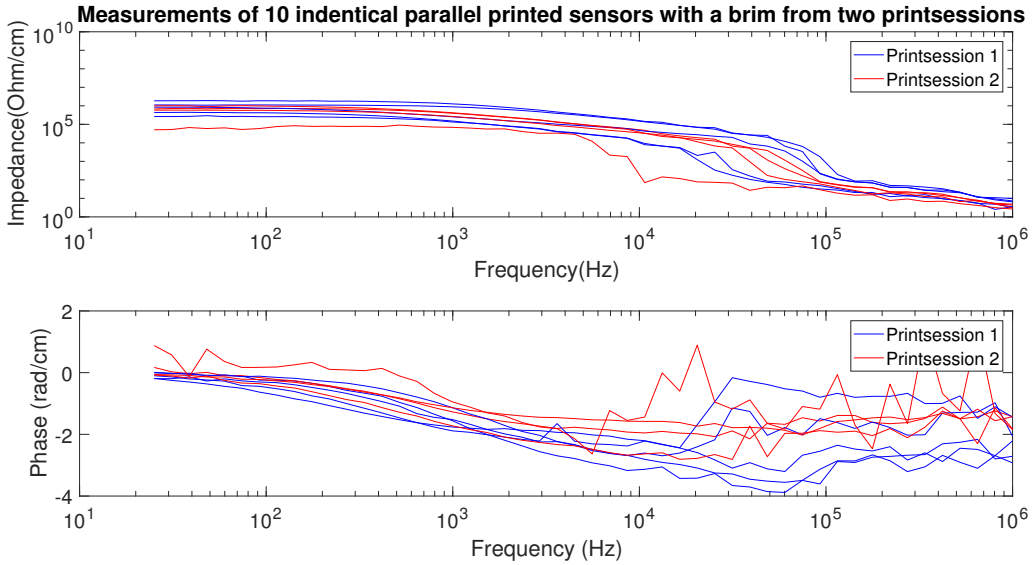

Figure 6.1: Impedance and phase measurement of force sensors printed with a parallel infill with a brim.

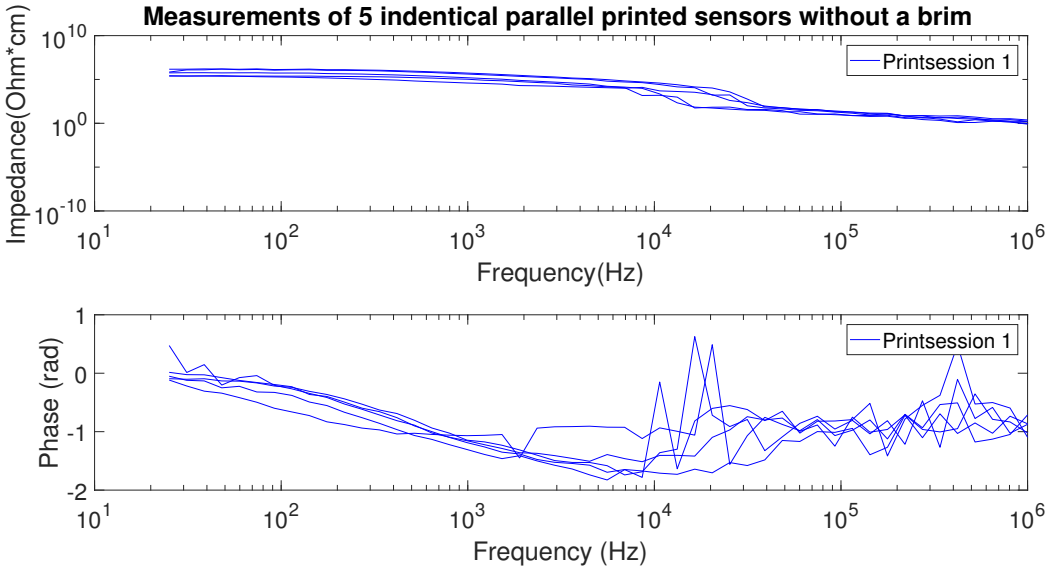

Figure 6.2: Impedance and phase measurement of force sensors printed with a parallel oriented infill without a brim.

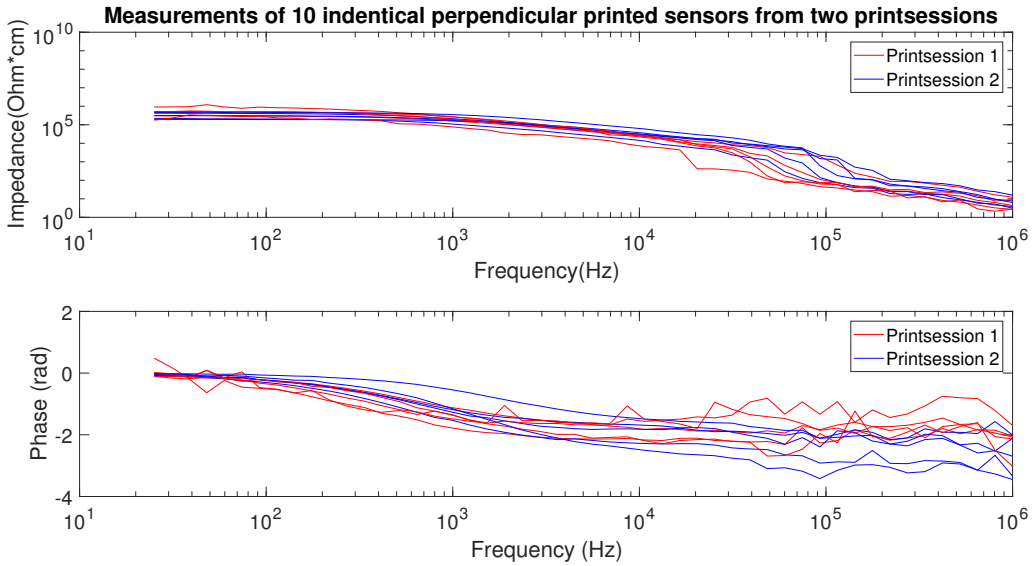

Figure 6.3: Impedance and phase measurement of force sensors printed with a perpendicular oriented infill.

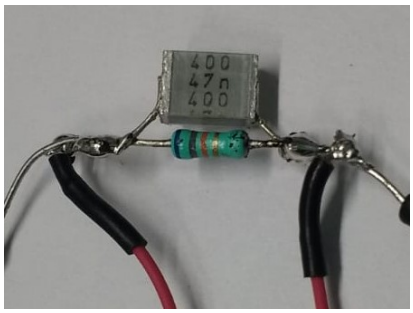

Figure 6.4: A capacitor and a resistance soldered together.

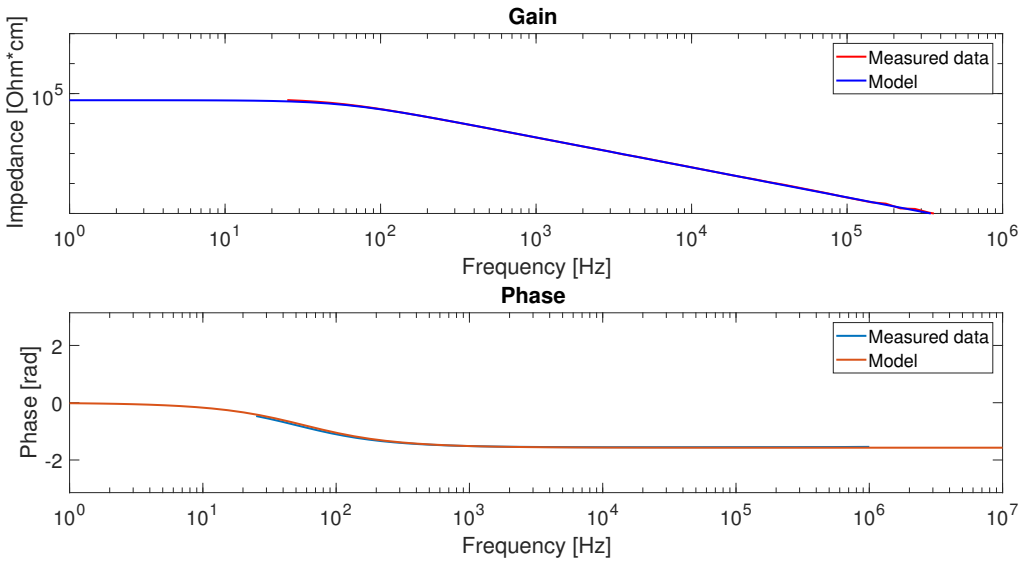

Figure 6.5: The measured data of the combined force sensor fitted with a frequency response $60\,\mathrm{k}\Omega$ and $290\,\mathrm{nF}$.

Table 6.1: Normalised values following from the mean impedance and phases.

Infill pattern	*capacitance*	*Resistivity*
Parallel	4 nF	780 kΩ cm
Parallel with brim	1.8 nF	730 kΩ cm
Perpendicular	4.6 nF	370 kΩ cm

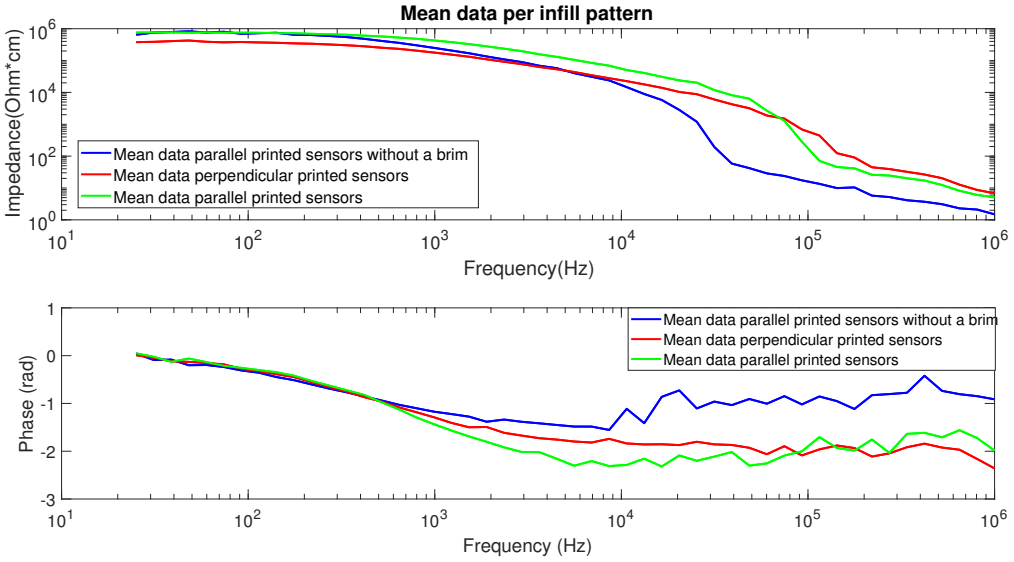

Figure 6.6: The means of the three infill oriented prints.

6.2 Contact interfaces

For the contact interface measurements in total 16 test structures are printed. 10 structures are printed for the connections which affect the material, they change the material while mounting the connections to the test structure. Six structures are printed for measuring the connections which do not affect the material, these connections do not use heat or other manners to affect the material while mounting to the test structure. The difference in numbers is due to the time consuming factor, the connections which do not affect the material take a lot of time to make.

For consistency all the test structures used have a perpendicular oriented infill pattern. The test structures are one-layered with a layer height of 200 µm and printed on a polyamide film. The test structures are measured in a four point measurement with the middle two voltage leads 1 cm apart. The LCR meter measured the impedance and phase at 50 frequencies between the 20 Hz to 1 MHz in two sweeps.

To measure the contact resistance, the mean impedance between 10 Hz to 100 Hz is determined. These values are converted to the contact resistance, as is described in Section 5.1.1. The contact resistances of all the connections are shown in Table 6.2. These resistances are compared to each other and plotted in a box plot, which is shown in Fig. 6.7.

In the box plot it is easily seen that the copper clip connection causes the lowest contact resistances and the braid connection causes the highest contact resistance. The measured data from the copper wire and header pin connection give fairly similar results. This makes it difficult to give a clear and reliable conclusion on which contact interface of these two causes the lowest contact resistance.

Table 6.2: The contact resistances of the different contact interfaces.

	Copper wire (Ω)	Headerpin (Ω)	Clip (Ω)	Braid (Ω)
Test structure 1	$5.02 \cdot 10^5$	$2.33 \cdot 10^5$	$3.15 \cdot 10^4$	$2.67 \cdot 10^6$
Test structure 2	$4.21 \cdot 10^5$	$2.71 \cdot 10^5$	$5.07 \cdot 10^2$	$1.35 \cdot 10^6$
Test structure 3	$1.53 \cdot 10^5$	$4.76 \cdot 10^5$	$2.59 \cdot 10^4$	$2.03 \cdot 10^6$
Test structure 4	$1.31 \cdot 10^5$	$2.61 \cdot 10^5$	-	-
Test structure 5	$9.67 \cdot 10^4$	$2.83 \cdot 10^5$	-	-

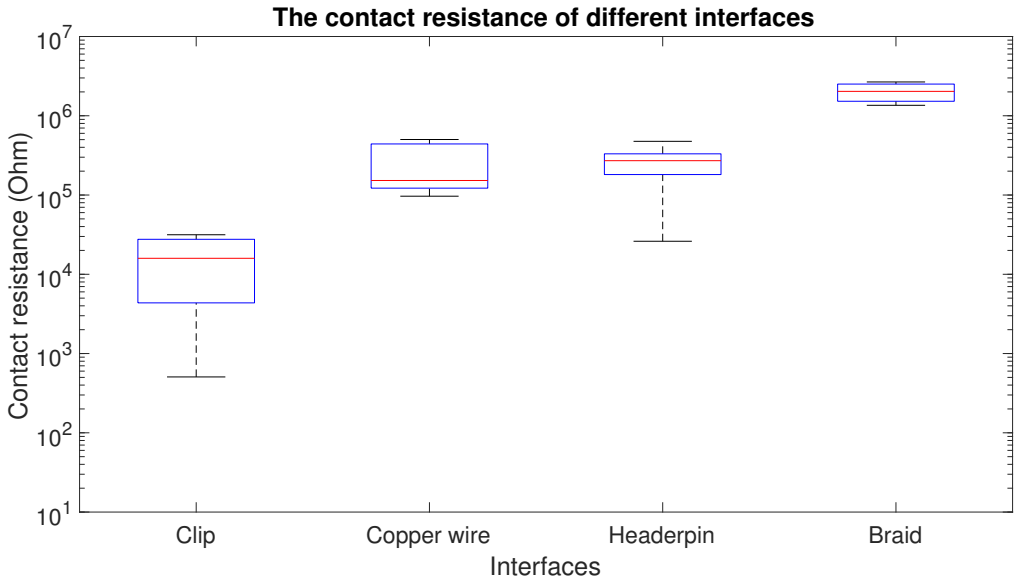

Figure 6.7: Boxplot of the different contact interfaces.

As stated earlier, the way copper wire and header pin connections are mounted could possible cause damage to the material. This can be confirmed, as is shown in Fig. 6.8 and Fig. 6.9. The heating process causes damage to the material surrounding the connection. This could cause the test structure to not function properly. Not only do these connections damage the material, the mounting of the header pin does not always go as wanted. Due to the size of the header pin, the header pin will easily get loose from the test structure. The copper wire connection has to deal less with this problem due to the diameter difference.

Figure 6.8: Impact of the header pin to the test structure.

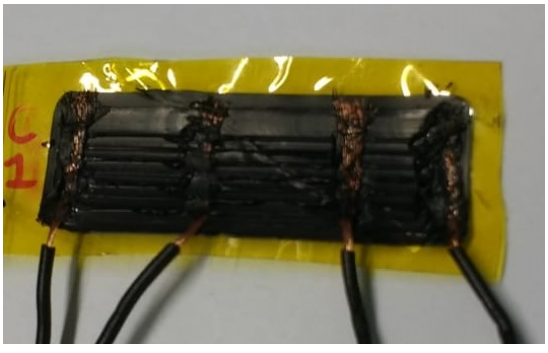

Figure 6.9: Impact of the copper wire to the test structure.

6.3 Two-layered force sensors

Two two-layered force sensors are printed. One sensor with two layers with the same perpendicular oriented infill (which is concluded from Section 6.1). The other sensor has two layers with a different oriented infill, namely perpendicular and parallel with a brim, as can be seen in Section 3.3.1. These sensors are mounted to a plate where a linear actuator applies force to the sensor while a LCR meter measures the capacitance and resistance of the force sensor.

The measurements are done multiple times and the testing setup was be built multiple times to make sure that the measurement conditions is reliable. For the measurements, the linear actuator applies force in steps of 2 N from 1 N to 10 N. The frequency applied in the measurement depends on the corner frequency of the sensor. The applied frequency for the same printing oriented force sensor is 100 kHz. The applied frequency for the different printing oriented force sensor is 10 kHz. The measurement mode is set to parallel, this is recommended in the manual for impedance measured higher than 10 kHz. The finished measurement for the same oriented infill force sensor is shown in Fig. 6.10. What can be seen is that the capacitance and resistance decreases, which is not expected. The capacity decreases with steps of 50 pF while the force increases by 2 N

The finished measurement for the different oriented infill force sensor is shown in Fig. 6.11. When compared to Fig. 6.10, quite some differences are present. The capacitance of the different oriented infill force sensor is also decreasing while the applied force is increasing but the steps are not as distinguishable as in Fig. 6.10. The capacity decreases with steps of 5 pF while the force increases by 2 N, which is 10 times smaller in comparison with the the same oriented infill force sensor.

The resistance of the different oriented infill force sensor is increasing while the applied force is increasing, which is totally different from Fig. 6.10, where the resistance decreased.

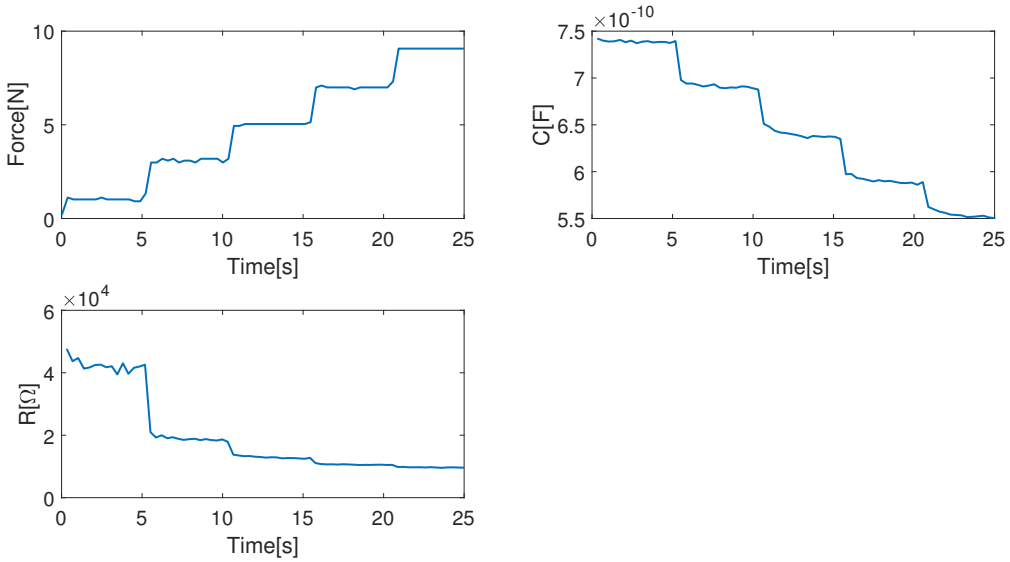

Figure 6.10: **Same oriented infill printed force sensor** Top-left: force plotted versus time, Top-right: capacitance plotted versus time, Bottom-left: resistance plotted versus time.

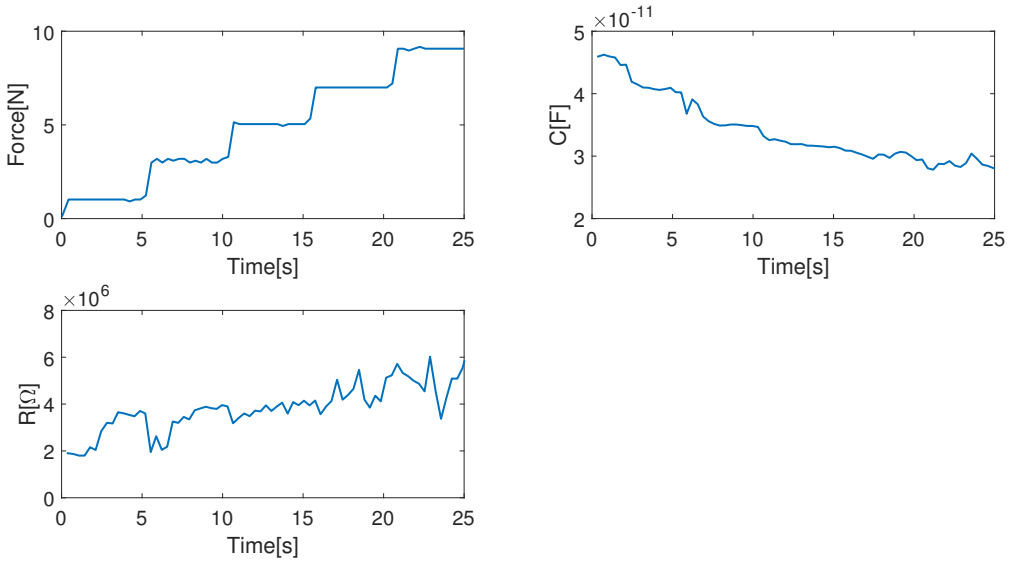

Figure 6.11: **Same oriented infill printed force sensor** Top-left: force plotted versus time, Top-right: capacitance plotted versus time, Bottom-left: resistance plotted versus time.

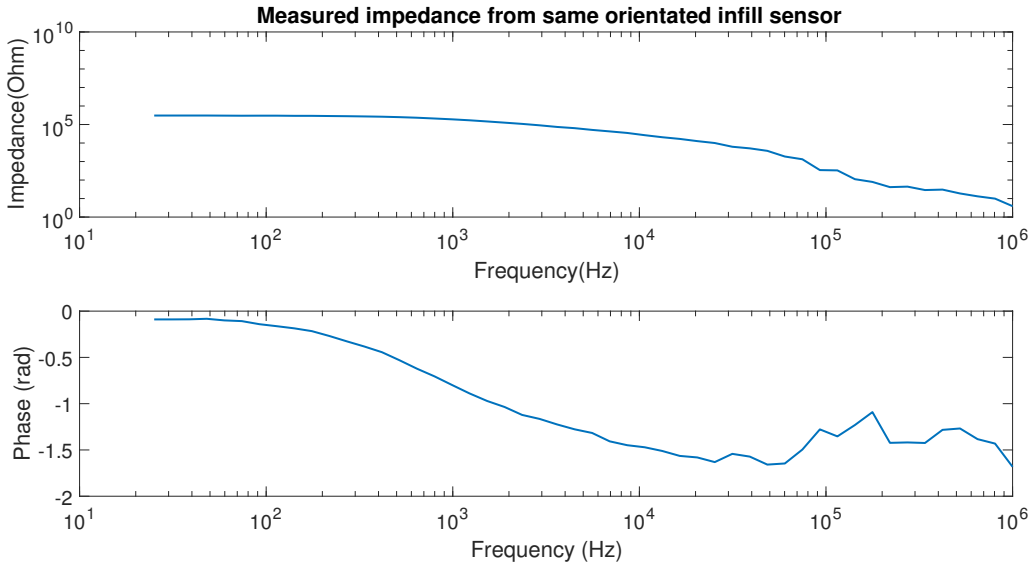

Figure 6.12: Impedance plot of the same oriented infill printed two-layered force sensor.

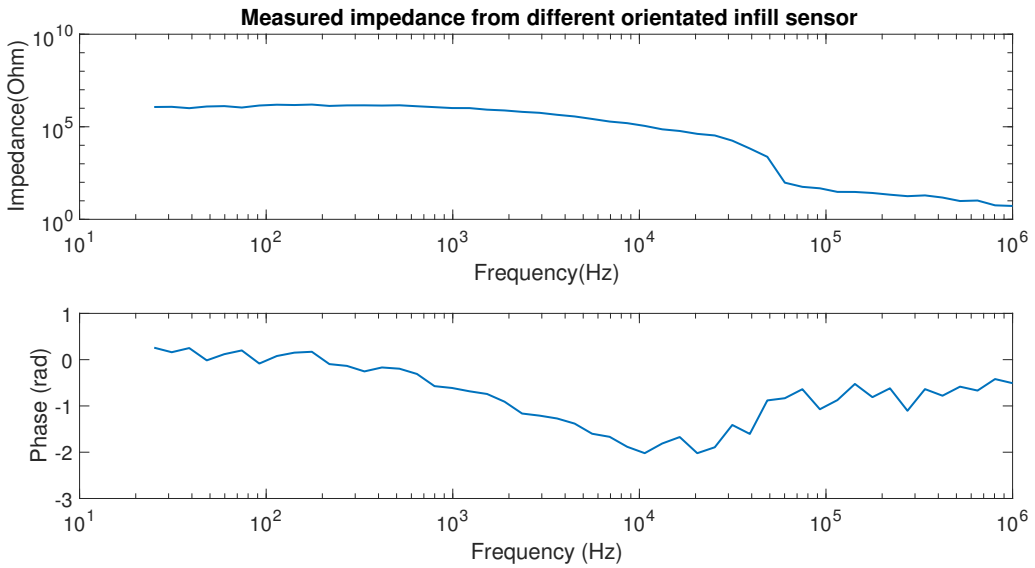

Figure 6.13: Impedance plot of the different oriented infill printed two-layered force sensor.

6.3.1 Linear actuator tip deformation

In the linear actuator a tip is used to apply force onto the sensor. The original tip has a round form, which is not ideal. To uniformly apply pressure to the sensor, a sensor tip of the same size as the sensor was needed. So the original tip is replaced with a self made tip made from PVC. To make sure the new tip does not deform more than the original tip, measurements were done where the tip pressed against a stable plate while applying an increasing force from 1 N to 10 N with steps of 2 N every 5 seconds. The results are shown in Fig. 6.14 and Fig. 6.15. The difference of deformation per force shift are shown in Table 6.3 where it is clear that the total deformation of both tips is the same.

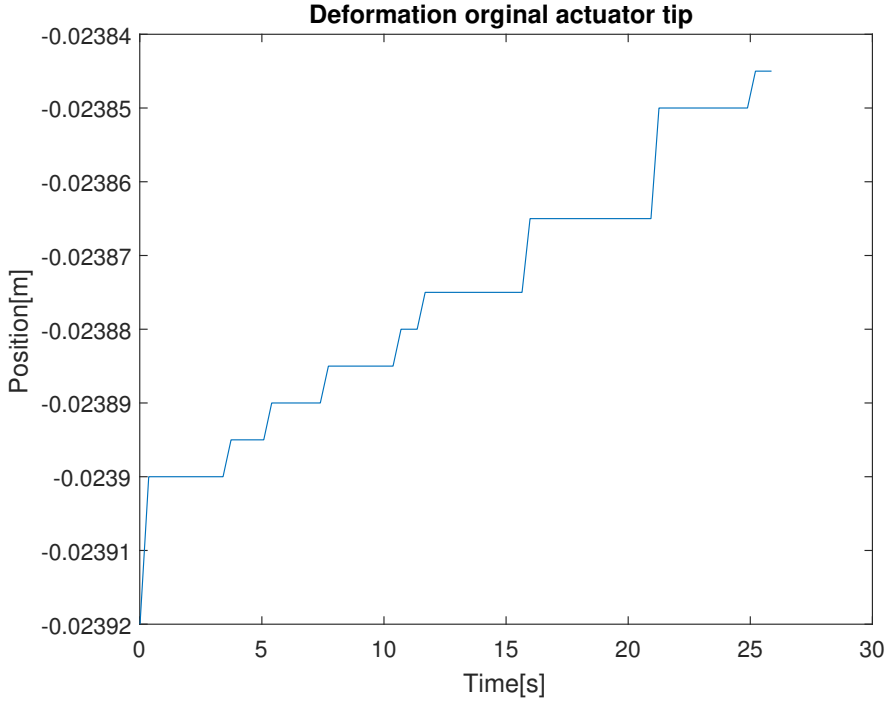

Figure 6.14: Position plot of the original tip where the force is increased 2 N every 5 seconds.

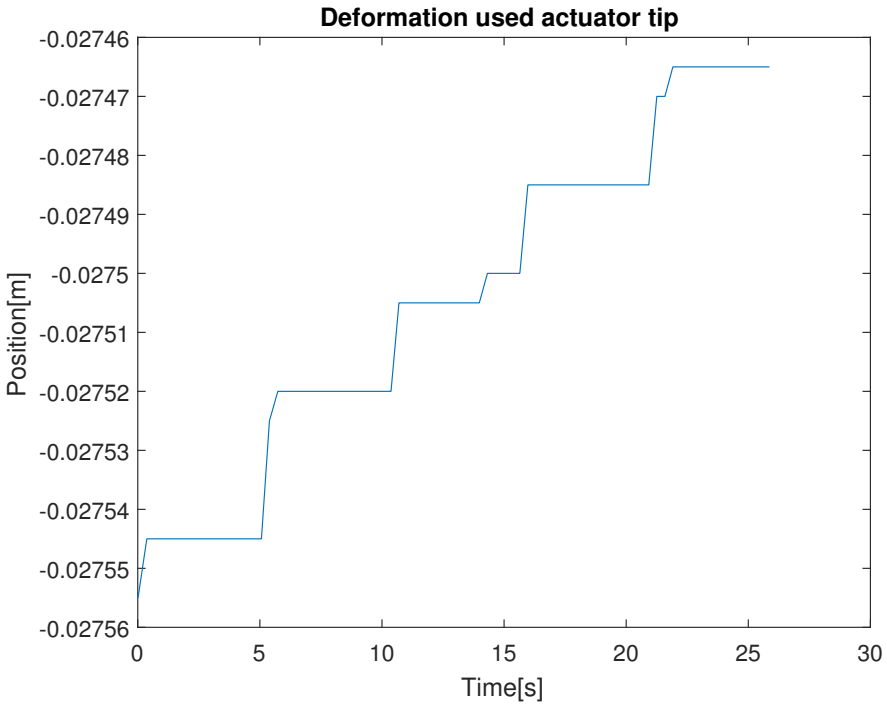

Figure 6.15: Position plot of the original tip where the force is increased 2 N every 5 seconds.

Table 6.3: Deformation tips of the linear actuator per 2 N applied.

	Orginal tip	**Used tip**
0 N to 1 N	0.2 µm	0.2 µm
1 N to 3 N	0.1 µm	0.1 µm
3 N to 5 N	0.1 µm	0.1 µm
5 N to 7 N	0.1 µm	0.1 µm
7 N to 9 N	0.2 µm	0.2 µm
Total deformation	0.7 µm	0.7 µm

Chapter 7

Discussion

All the created sensors are printed by a 3D printer, with the test structures which are compared all printed at the same time. This should exclude the impact of the surface but instead introduces another possible variance in the sensors. The test structures are all printed at the same time, which causes that they are all printed on a different location on the printing bed. If the levelling of the printing bed is not uniform, the sensors are printed with varying height distances between the extruder head and the printing bed. The connections to the sensors and test structures are mounted by hand, which could cause human errors which affect the measurements.

All the measurements done on the LCR meter follow the form of the presented model until the frequency reaches 10 kHz when the similarity stops and the data takes its own path with a different slope than the model. This is clearly visible in Appendix B where a model is fitted over the measured data. To make sure this behaviour is not caused by the LCR meter, measurements have been done on a parallel capacitor and resistor. These measurements did follow the model nicely, even around 10 kHz. So the problem is caused by the test structure. To make sure the behaviour is not caused by a specific kind of infill pattern, contact interface or number of layers, all the measurements done are compared and analyzed. In all measurements the same behaviour is seen around 10 kHz. The only thing all the test structures have in common is the material they are made from, so it can be concluded that this phenomenon is due to the 3D printed material and not caused by the contact interfaces, infill pattern or number of layers.

As stated in the Introduction, assumed is the distribution of conductive carbon particles being inhomogeneous, with the highest concentration of particles being in the center of the filament. During the printing process, the filament is printed in a meandering structure, where the orientation of the infill decides the angle in which the meandering takes place. This causes not only a capacitance between the layers but also in the layer itself. When current flows through the printed layer, it will most likely follow the path in the printed filament where the highest concentration of carbon particles is. This would mean that the resistance of the current flowing trough the perpendicular oriented infill pattern is lower than the other two infills, which is true according to the measurements done. Two types of parallel oriented infill patterns are compared, one with a brim and one without a brim. The resistance of the infill with a brim will probably be lower, because the current can flow easily through the brim. This is supported by the results from the measurement, where the resistance of the infill with a brim is lower than the resistance of the infill without a brim. What was not expected is that the measured capacitance is the higher in the parallel infill with a brim than the parallel infill without a brim with a factor two. The value of the measured capacitance of the parallel oriented infill pattern lays closer to the value of the measured capacitance of the perpendicular oriented test structure than the parallel oriented infill pattern with a brim. The high capacitance in the parallel oriented infill with a brim could be due to the capacitance between the brim and the parallel infill pattern, which is a 90 degrees change in the infill patterns. This cause these layers to not be connected at all with the high capacitance as result.

In comparison with the perpendicular oriented infill pattern, current flowing through the parallel oriented infill pattern has probably to deal with a higher resistance because the shortest way for the current to flow is perpendicular to the orientation of the printed filament. With the assumption of the inhomogeneous distribution in mind, it will most likely act as a lot of small capacitors in series with each other. This

would cause a high resistance. The results generated from the measurements indeed see a lower parallel resistance in the perpendicular oriented infill pattern which differs with a factor two from the parallel oriented infill patterns.

The intention of this research was to fabricate a capacitive force sensor, where the capacitance would change when external force is applied. With the formula for a parallel plate capacitor in mind the assumption was made that the capacitance would increase when an external force was applied. The results from the measurements where external force was applied to the two-layered force sensors showed something else. The capacitance decreased while the applied force increased. This implies that the force sensor does not function like a parallel plate capacitor. Two force sensors were compared, one with the two layers with the same orientation and one with two layers with a different orientation. In both force sensors the capacitance decreased when force was applied, but the difference is in the resistance. In the two-layered sensor with the same orientation the resistance decreased and in the two-layered sensor with a different orientation the resistance increased. As stated in the Introduction, due to the filament being printed in an oval form the surface of a printed layer has a wavy structure. When two layers with the same orientation and the same wavy structure are pressed together, the highest points of the wavy structure press on each other which cause a change in the volume and in the distribution of carbon particles. This could cause less resistance. When two layers with a different orientation are pressed together, the lowest point of the wavy structure press together with the high points of the wavy structure. This causes that the volume stays approximately the same and the resistance to increase.

The decrease in capacitance could be due to different reasons. When force is applied the sensor becomes broader and thinner because the volume stays the same, this changes the distribution of carbon particles again. When the concentration carbon particles becomes more uniform in the material and exceed the turning point in the percolation theory, it could cause better conductance. This could cause the electrical charge which normally is stored in the capacitor, become dielectric leakage because the material is not a perfect isolator. Future research should give more clarity about the distribution of carbon particles and what happens when force is applied.

Chapter 8

Conclusion

In this report research has been done with the goal to create a force sensitive capacitance sensor with the use of the inhomogeneity in 3D printed material. The possible cause of these inhomogeneities in the material is the inhomogeneous distribution of carbon particles. Concluded is that these inhomogeneities could make printed structures made from carbon doped thermoplastic polyurethane material function as a capacitor. After the table of requirements was finished, it showed that research had to be done. This research is done on one-layered test structures where the impact of the infill patterns tested was measured. This is done by measuring the parallel resistance of the different types of infill. These measurements showed that the infill does have an impact on the parallel resistance. The perpendicular to the contact interface oriented infill gave the lowest parallel resistance, which makes it the best infill pattern for the two-layered test force force sensors. The error bar of the perpendicular oriented infill sensors was also the smallest, which means that these measurements were the most consistent. There were also two types of parallel to the contact interface oriented infills compared where one had a brim around the parallel infill pattern and one did not. What can also be concluded from these measurements is that the brim around the force sensor decreases the resistivity of the force sensor by $50\,\mathrm{k}\Omega$. This is what was expected with the inhomogeneous distribution theory in mind, which stated that concentration of conductive carbon particles is the highest in the middle of the printed filament. Which means that current flows easier through the brim instead of flowing through the infill pattern which is meandering.

Research on the contact resistances of different contact interfaces were also done. For the contact resistance the copper clip connections gave the lowest contact resistance. The braid connection gave the highest contact resistance.

The deformation of the tip used in the linear actuator to apply force is also measured and compared with the original tip. The results show the same total deformation. This means this tip can be used to apply force without worrying about unwanted deformation.

The measurements done with the two-layered force with the same printing orientation sensor showed that the capacitance decreases when applied force increases. This was not what was expected, but the capacitance does change when force is applied. The two-layered force sensor with different printing orientations did not function as expected. The capacitance change was on a smaller scale than the capacitance change of the force sensor with two layers with the same orientation. Based on the observations and measurements the two-layered force sensor with two layers with the same printing orientation show potential to function as a capacitive force sensor. However further research needs to be done.

8.1 Recommendations

In order to develop a working capacitive force sensor more research on the composition of the filament is needed. This is needed to better understand the distribution of the carbon particles instead of making assumptions, for example by using a scanning electron microscope. Another factor that is not researched is the influence of the surface area of the sensors. This could have an influence on the

parallel resistance. All the measurements done used test structures consists off one printed layer and the force sensors consisting of two layers. It could be interesting to see how the sensor would function with multiple layers. And finally, the measurements used only 50 frequency points between 20 Hz and 1 MHz to measure because this took less time. This causes the plot of the results to become less smooth. For better plots with smoother lines, there is recommended to use more frequency points in the measurements. And finally, for future two point measurements, it is recommended to use copper clips for the connection to a current.

Appendix

Appendix A: All used one-layered test structures

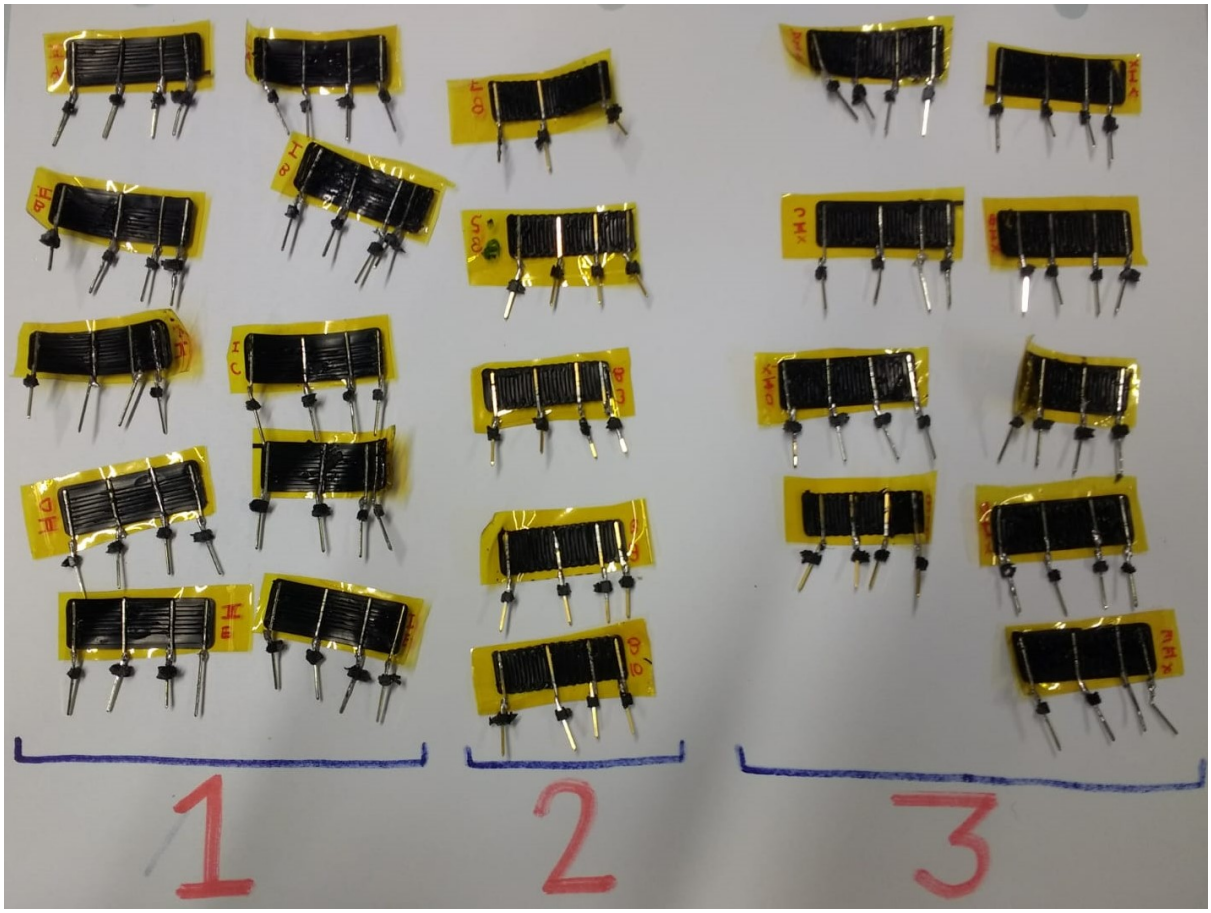

Figure 1: **All test structures used for measuring parallel resistance** 1: perpendicular test structures, 2: parallel test structures without a brim, 3: parallel test structures with a brim

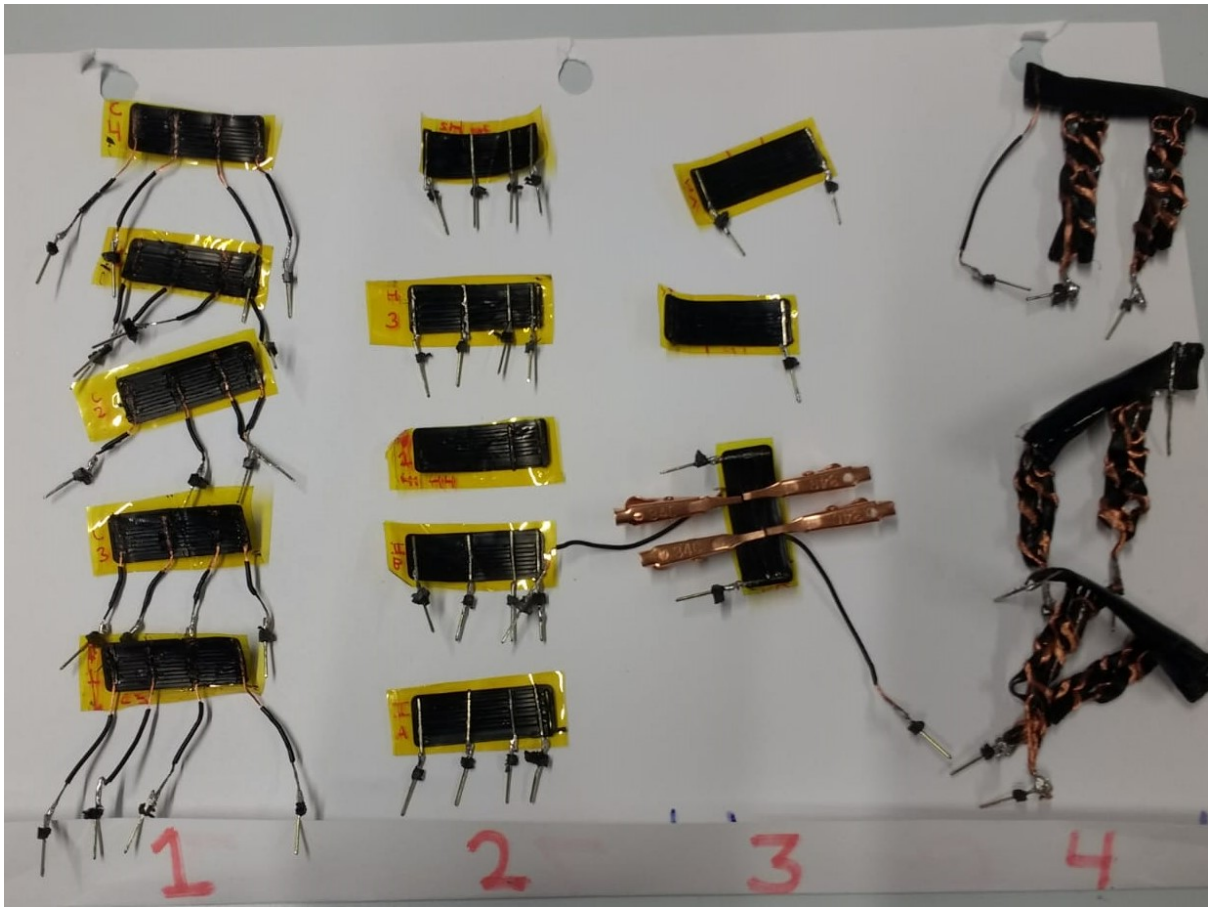

Figure 2: **All test structures used for measuring contact resistance** 1: copper wire interface, 2: headerpin interface, 3: copper clips interface, 4: braid interface

Appendix B: The errorbars of the infill measurements.

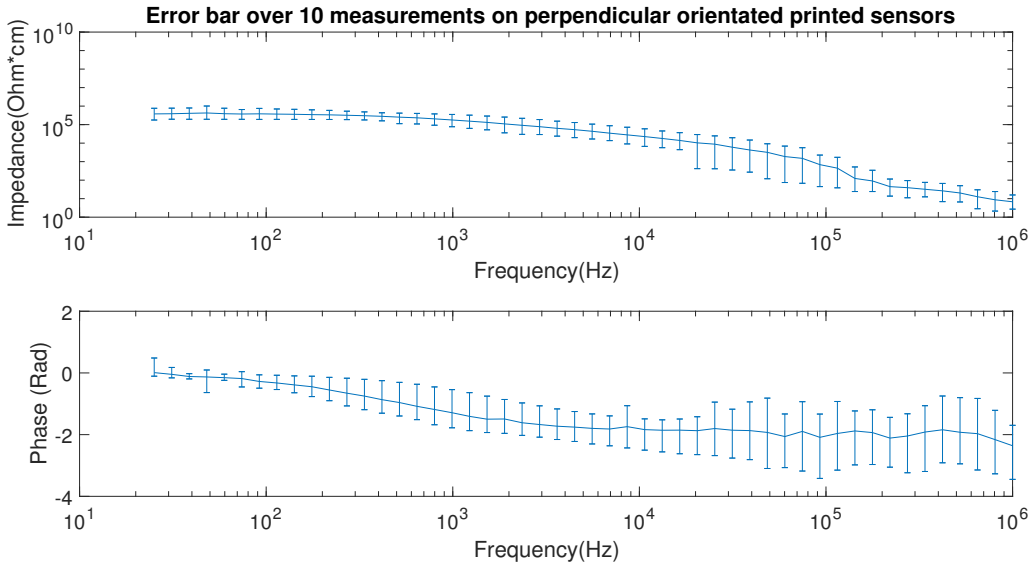

Figure 3: Error bar of the perpendicular oriented test structures (measurements from 10 test structures)

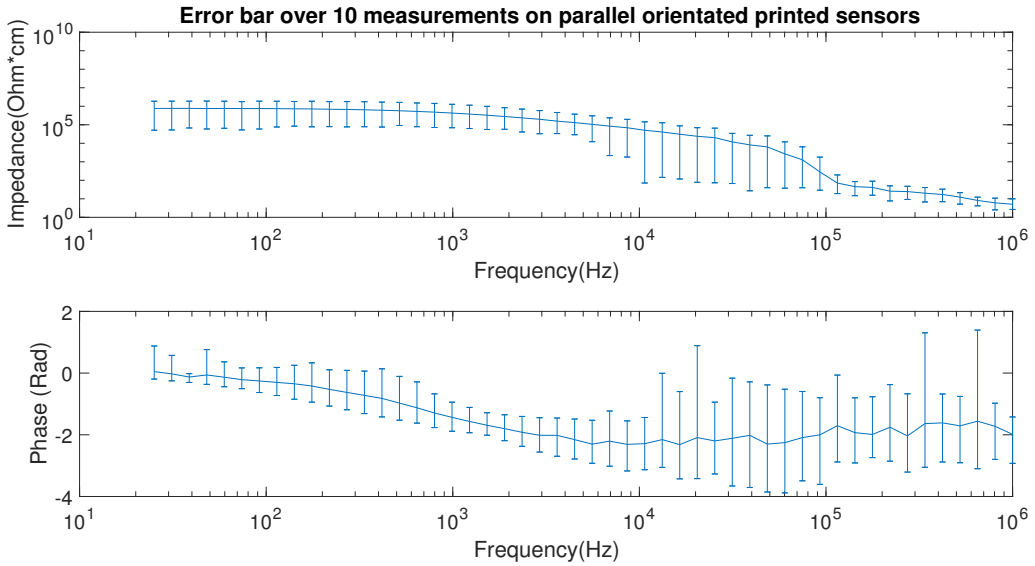

Figure 4: Error bar of the parallel oriented test structures with a brim (measurements from 9 test structures)

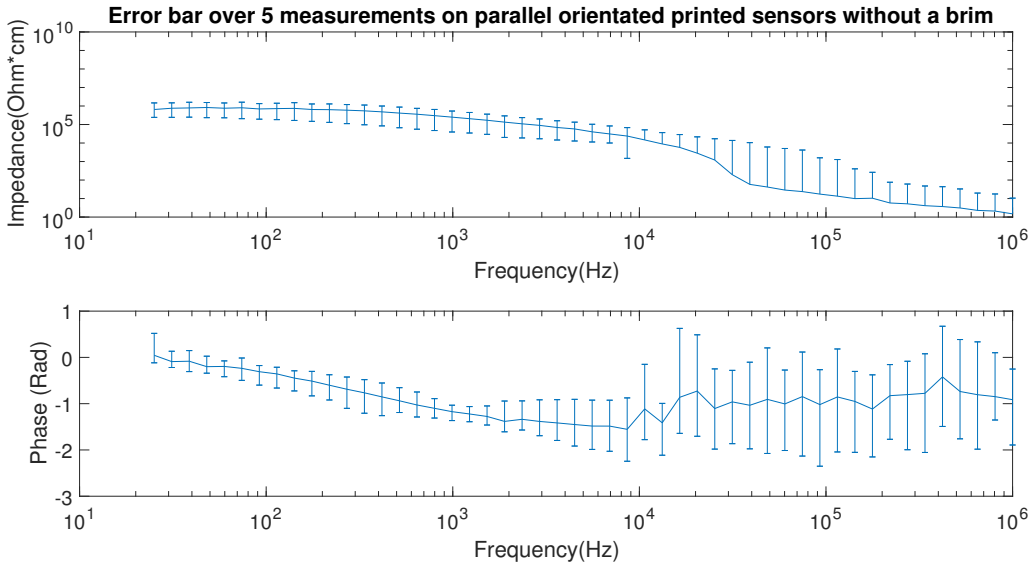

Figure 5: Error bar of the parallel oriented test structures without a brim (measurements from 5 test structures)

Appendix C: The measured impedance data with the frequency response fitted over the data.

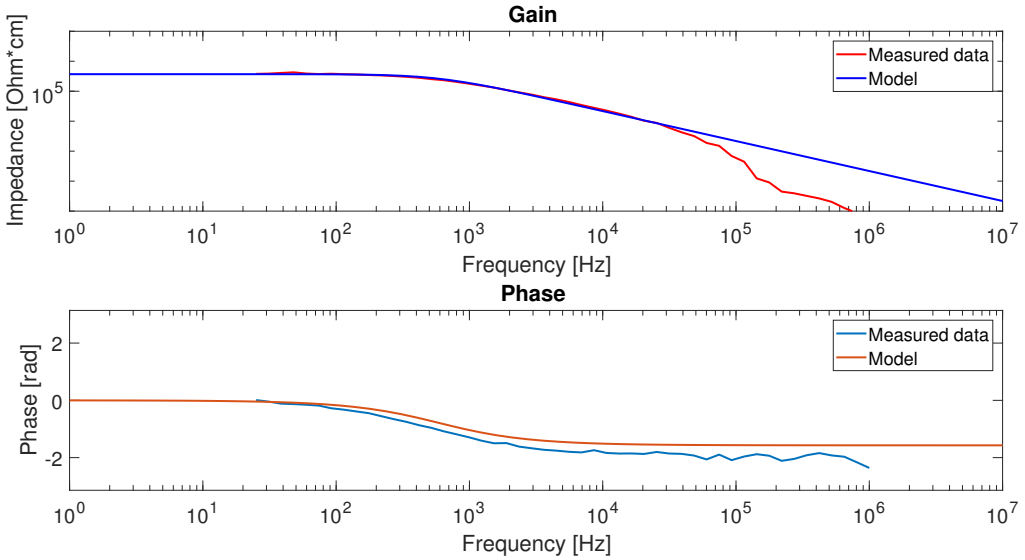

Figure 6: The frequency response fitted over the mean data of the perpendicular oriented test structures with a brim.

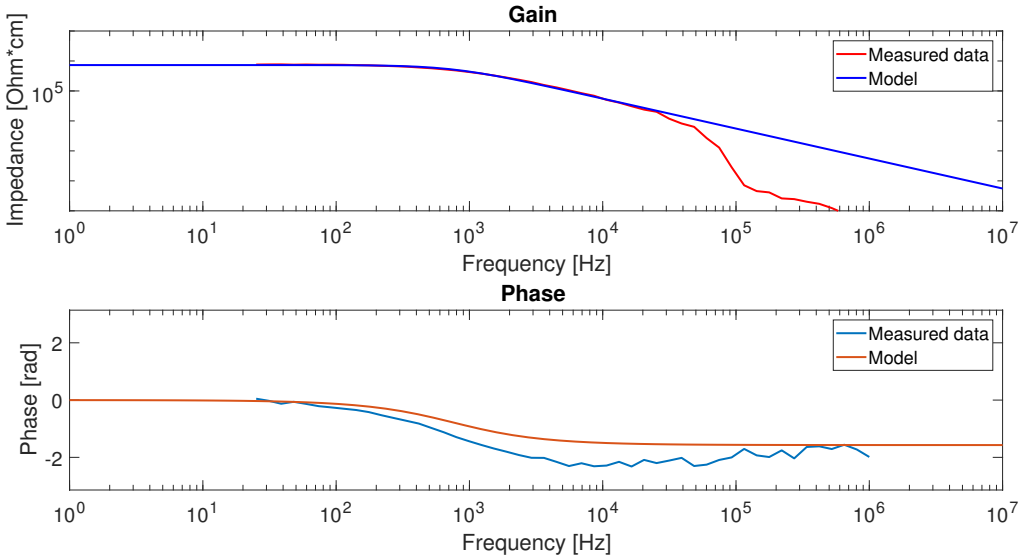

Figure 7: The frequency response fitted over the mean data of the parallel oriented test structures with a brim.

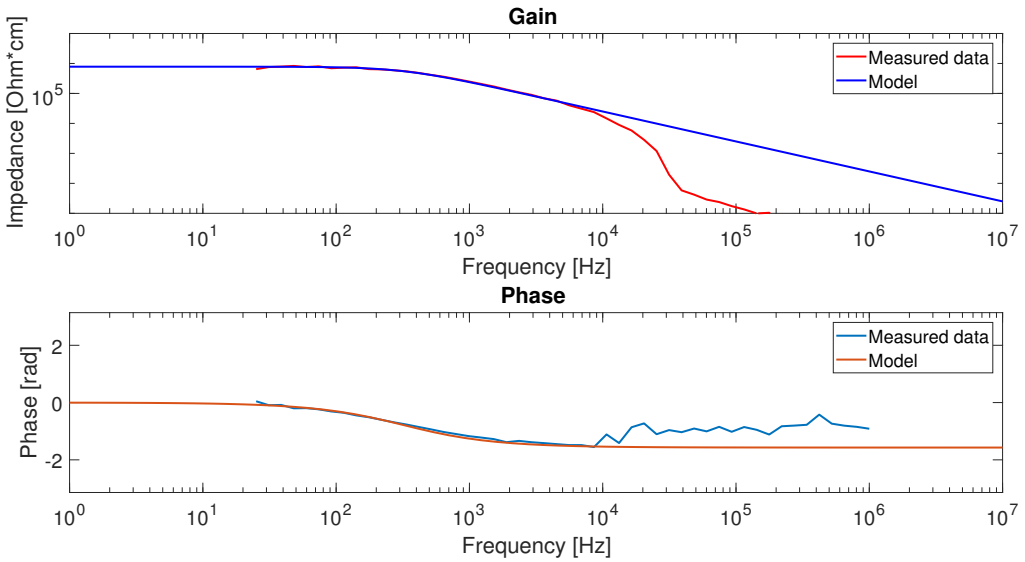

Figure 8: The frequency response fitted over the mean of the measured data from of the parallel oriented test structures without a brim.

Appendix D: All slicer images used for printing the sensors

One-layered sensors

Infill sensors

The one-layered sensors used for the measuring the parallel resistance of the different infill patterns use three infill patterns. Perpendicular oriented infill pattern, parallel oriented infill pattern with a brim and parallel oriented infill pattern without a brim as seen in Fig. 9, Fig. 10 and Fig. 11. These are printed with a layer height of 200 µm. The further dimensions are shown in Fig. 12.

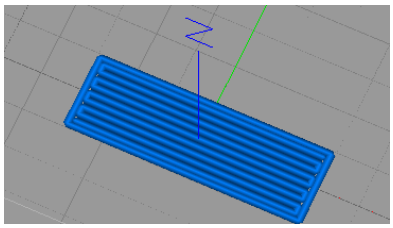

Figure 9: Perpendicular oriented infill pattern.

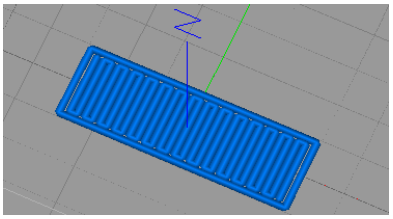

Figure 10: Parallel oriented infill pattern with a brim.

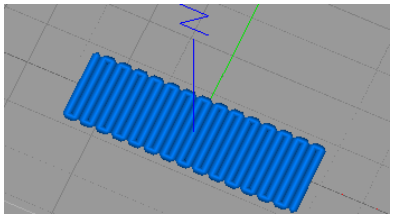

Figure 11: Parallel oriented infill pattern without a brim.

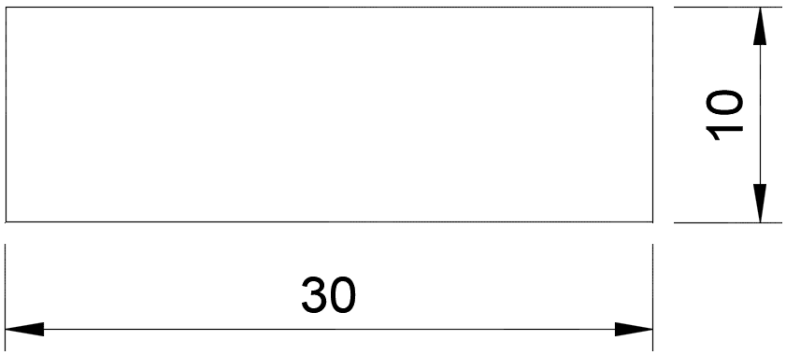

Figure 12: Drawing of CAD model of the one-layered test structure. The dimensions are in millimeters.

Contact interfaces

For the contact interfaces the one-layered test structure with a perpendicular oriented infill as shown in Fig. 9 is used. Only for the braid interface a new test structure is printed, as shown in Fig. 14. These are printed with a layer height of 200 µm. The further dimensions are shown in Fig. 13.

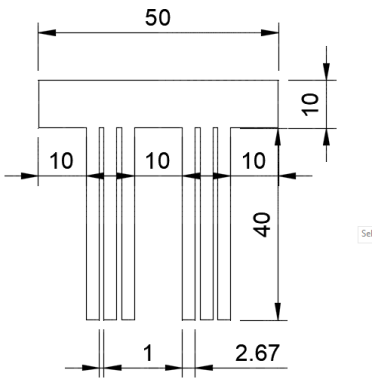

Figure 13: Fusion360 model of the test structure with the dimensions in millimeters.

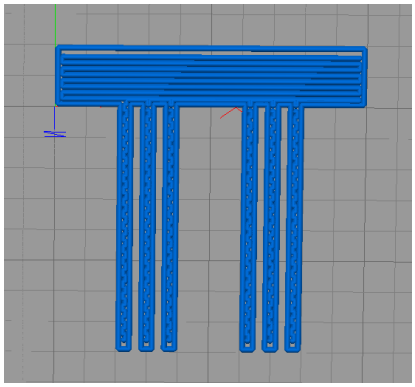

Figure 14: The test structure with the printing orientation.

Two-layered sensors

For the two-layered force sensor consist of two layers which with a layer height of 200 µm. The slicer images are shown in Fig. 15 and Fig. 16. The further dimensions are shown in Fig. 17.

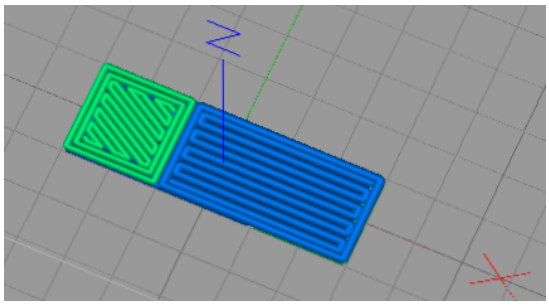

(a) Layer one of two

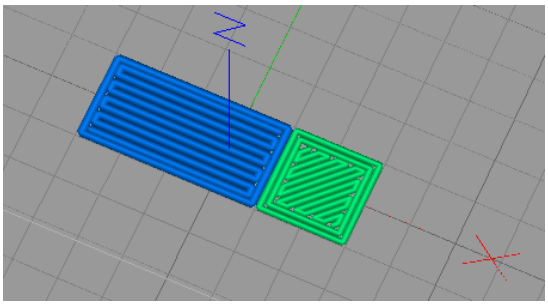

(b) Layer two of two

Figure 15: A slicer model of the same oriented printed two-layered force sensor. The green represents the Ninjaflex and the blue the ETPU.

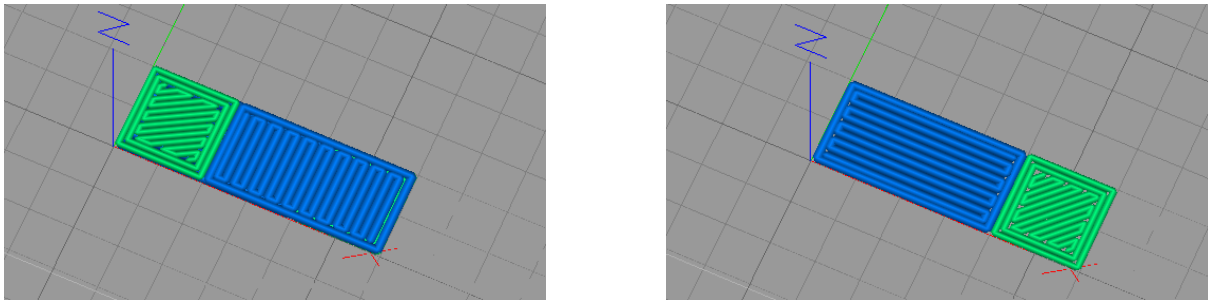

(a) Layer one of two

(b) Layer two of two

Figure 16: A slicer model of the different oriented printed two-layered force sensor. The green represents the Ninjaflex and the blue the ETPU.

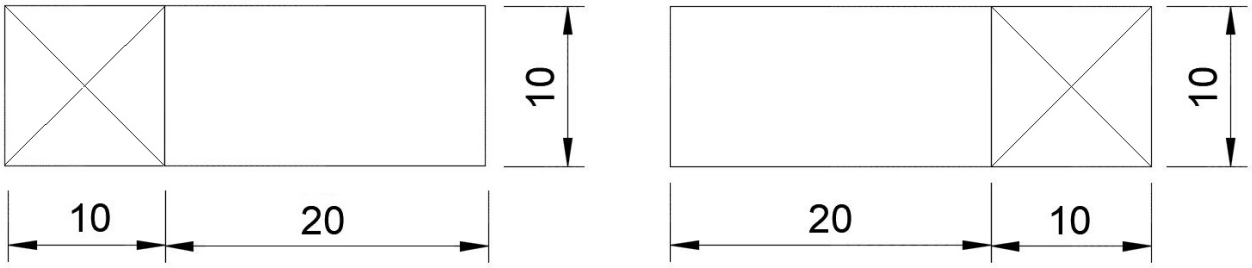

(a) Layer one of two.

(b) Layer two of two.

Figure 17: Drawing of the CAD model of the two-layered force sensor with the dimensions in millimeters and the height of the structure is $0.2\,\mathrm{mm}$. The ares with the cross represents the dielectric material and the open areas represent the carbon filled thermoplastic polyutherane.

Recommended Reading

[1] Varotsis, A. (n.d.). *Introduction to FDM 3D printing.* Retrieved June 24, 2018, from https://www.3dhubs.com/knowledge-base/introduction-fdm-3d-printing

[2] Eijking, B., Sanders, R., and Krijnen, G. (2017, October). *Development of whisker inspired 3D multimaterial printed flexible tactile sensors.* In SENSORS, 2017 IEEE (pp. 1-3). IEEE.

[3] Schouten, M., Sanders, and ., Krijnen, G. (2017, October). *3D printed flexible capacitive force sensor with a simple micro-controller based readout.* In SENSORS, 2017 IEEE (pp. 1-3). IEEE.

[4] Saari, M., Xia, B., Cox, B., Krueger, P. S., Cohen, A. L., and Richer, E. (2016). *Fabrication and Analysis of a Composite 3D Printed Capacitive Force Sensor.* 3D Printing and Additive Manufacturing, 3(3), 136-141.

[5] *Material info : PI-ETPU 95-250 Carbon Black.* (n.d.). Retrieved June 27, 2018, from https://rubber3dprinting.com/pi-etpu-95-250-carbon-black/

[6] Wolterink, G., Sanders, R., Muijzer, F., van Beijnum, B. J., and Krijnen, G. (2017, October). *3D-printing soft sEMG sensing structures.* In SENSORS, 2017 IEEE (pp. 1-3). IEEE.

[7] Valentine, A. D., Busbee, T. A., Boley, J. W., Raney, J. R., Chortos, A., Kotikian, A., ... and Lewis, J. A. (2017). *Hybrid 3D printing of soft electronics*. Advanced Materials, 29(40).

[8] Kanbur, Y., and Kkyavuz, Z. (2009). *Electrical and mechanical properties of polypropylene/carbon black composites.* Journal of Reinforced Plastics and Composites, 28(18), 2251-2260.

[9] Hobert, E. (2017, June). *3D Printed Flexible Fingertip Strain Sensor*

[10] *Overview of Two-Wire and Four-Wire (Kelvin) Resistance Measurements* (n.d.). Keithley Instruments. Retrieved June 28, 2018 from http://www.twek.com

[11] Palmiga Innovations. *Material info for pi-etpu 95-250 carbon black.* Retrieved June 28, 2018 from http://rubber3dprinting. com/pi-etpu-95-250-carbon-black/

[12] Ninjatek. *Ninjaflex 3d printing filament technical specifications.* Retrieved June 28, 2018 from https://ninjatek.com/ wp-content/uploads/2016/05/NinjaFlex-TDS.pdf.

[13] Wire, Stranded, Flexivolt E, Hi Flex, PVC, Black, 27 AWG, 0.1 mm, 328 ft, 100 m. (n.d.). Retrieved June 29, 2018, from http://nl.farnell.com/staubli/60-7001-21/wire-flexi-e-black-0-10mm/dp/4326702

[14] MICRO ALLIGATOR CLIP, 5A, 5.6MM. (n.d.). Retrieved June 29, 2018, from http://uk.farnell.com/mueller-electric/bu-34m/micro-alligator-clip-5a-5-6mm/dp/2815063

[15] Kapton Tapes. (n.d.). Retrieved June 28, 2018, from https://www.kaptontape.com/

[16] Creator Pro 3D Printer. (n.d.). Retrieved June 28, 2018, from http://www.flashforge.com/creator-pro-3d-printer/

[17] Creator Pro 3D Printer. (n.d.). Retrieved June 28, 2018, from http://www.flashforge.com/creator-pro-3d-printer/

[18] Hewlett Packard. *HP 4284A PRECISION LCR METER OPERATION MANUAL*. Sixth Edition, August 1998.

[19] L.A. Bumm (Phys2303) *AC steady-state circuits, AC impedance, RC, RL, and RLC filters*. (n.d.). Retrieved June 28, 2018, from http://www.nhn.ou.edu/ bumm/E-LAB/Lect_Notes/AC_impedance_v2_1_1.html

[20] Smac corporation. http://www.smac-mca.com/lca-series-p-15.html, Retrieved June 28, 2018